P-04-196

Oskarshamn site investigation

A deformation analysis of the Äspö GPS monitoring network from 2000 to 2004

Lars E. Sjöberg, Ming Pan, Erik Asenjo
Royal Institute of Technology
Department of Infrastructure

May 2004

Svensk Kärnbränslehantering AB
Swedish Nuclear Fuel
and Waste Management Co
Box 5864
SE-102 40 Stockholm Sweden
Tel 08-459 84 00
+46 8 459 84 00
Fax 08-661 57 19
+46 8 661 57 19

ISSN 1651-4416
SKB P-04-196

Oskarshamn site investigation

A deformation analysis of the Äspö GPS monitoring network from 2000 to 2004

Lars E. Sjöberg, Ming Pan, Erik Asenjo
Royal Institute of Technology
Department of Infrastructure

May 2004

Keywords: GPS, satellite, crustal deformation, faults.

Abstract

In the year of 2000 the Äspö GPS deformation network, consisting of seven stable sites within an area of 15x20 km was established for studying the feasibility of applying the satellite GPS technology to monitor possible small crustal motions in a local area. The goal is to be able to detect any crustal deformation exceeding 1 mm/yr after a few years of repeated observations, three times a year.

The baselines of the network vary from 2 to 7 km and the observation points are located on each side of two possible active faults. Each station has a steel benchmark, fixed in the bedrock, for the antenna mount. All observations analysed in this report were collected by Trimble 4000 SSE dual frequency Geodetic GPS receivers (with code and phase observables at two frequencies) and Dorne-Margolin choke ring antennas, which allow an optimum reduction of noise and multipath effects of incoming satellite signal.

In 2002, after the completion of six successful epoch GPS campaigns, the achieved results were analysed. As was expected, no significant crustal motions could be detected after such a short period of time, but the data quality seemed very good despite some extreme ionospheric disturbances of the signal propagation.

From October 2002 to March 2004 a second observation period, with five additional epoch GPS observation campaigns, followed. Unfortunately, ionosphere activities, characterised by a cycle of 11 years, were rather strong during all observation campaigns, reaching an overall maximum in 2002. Under normal circumstances the ionosphere bias should not influence the baseline determination of a small network, and this experience seems to hold rather well also for our data. The estimated precision of a site coordinate vs the fixed site Knip is of the order of 1.5-2 mm in the horizontal and 3-4 mm in the vertical for each epoch of observations.

From the two types of analyses (regression analysis of each baseline and a joint least squares adjustment of all the data) from the 11 GPS campaigns we conclude that 3 baselines change temporarily ca -1 ± 0.2 mm/yr. Site Kidr moves to the SSE at the rate of 1.5 mm/yr, site Stor to the SSV at 1.2 mm/yr, and site Karr moves to the NV at 1.3 mm/yr with respect to a selected fixed point. These motions may indicate that the two blocks rotate counter-clockwise, but this conclusion is not significant based on the present data.

These changes of 3 baselines and one site are statistically verified based on t-tests at the risk level of 5%. At the risk level of 1% all baselines and sites, except one of each, pass the tests for no motion. No vertical crustal motions were detected, but there is a sudden jump of 3 cm at one epoch and site. This change of level cannot be satisfactory explained.

There is a risk that the data is contaminated by some undetected systematic errors. In particular, the strong ionosphere bias may have influenced the results. In order to sort out this remaining problem, we recommend that the epoch observation campaigns continue a few more years, possibly extended to a full solar cycle. Fortunately, the ionosphere activity will calm down in the next few years, allowing even more reliable observations and evaluation of the data.

Sammanfattning

År 2000 uppdrog Svensk Kärnbränslehantering AB åt geodesigruppen vid Kungliga Tekniska högskolan i Stockholm att genomföra en försöksstudie vid Oskarshamns kärnkraftverk. Studien avser att undersöka tillämpningen av satellitsystemet GPS (Global Positioning System) för uppmätning av eventuella små rörelser i jordskorpan. Målet är att kunna detektera en rörelse som uppgår till åtminstone 1 mm/år inom några år av mätningar. För ändamålet upprättades ett geodetiskt nät om sju punkter inom ett område av 15x20 km, och avståndet mellan punkterna uppgår till 2-7 km. Området delas av två tektoniska svaghetszoner, och mätpunkterna har fördelats på de olika geologiska blocken. För att erhålla bästa möjliga geometriska konfiguration mot GPS-satelliterna har punkterna placerats på berg i dagen med god sikt i alla riktningar, i de flesta fall ända ner till 10 grader över horisonten. Varje mätpunkt definieras av en upptill gängad ståldubb fäst i ett borrhål, och på denna fästs en GPS-antenn.

Observationsstrategin har varit att mäta epokvis tre gånger per år. Vid varje mättillfälle har vanligtvis sju stycken geodetiska GPS-mottagare av typ Trimble 4000 SSE använts. En sådan mottagare observerar både kod- och fassignal på L1- och L2-frekvenserna. Brusnivån för kod- och fassignal är cirka 60 cm respektive 6 mm vid en dubbeldifferensmätning. För att minska inflytandet från systematiska fel, särskilt flervägsfel från reflekterande signaler, används en så kallad ”chokering-antenn” och varje mättillfälle utsträcks till 5 sessioner (dagar) i varje mätpunkt. Genom den dubbla frekvensmätningen på L1- och L2-signalerna kan det systematiska felet på grund av jonosfärsfördröjningen i hög grad modelleras och elimineras från mätresultaten.

Idag har deformationsnätet observerats under nästan fyra år vid totalt 11 tillfällen. Ur de mer än en miljon observationer som insamlas vid varje mätepok har punkternas koordinater noga utjämnats enligt minsta kvadratmetoden med en central punkt i området betraktad som en given punkt. Medelfelen i de utjämnade punktkoordinaterna vid varje mätepok är ca 1,5-2 mm i plan och 3-4 mm i höjd, och varje baslinje kan bestämmas med ett medelfel av ca 1–1,5 mm. Genom att analysera punkternas förändringar i tiden kan eventuella deformationer i jordskorpan prövas.

En första deformationsanalys avser förändringen av varje enskild baslinje, dvs. den lutande längden mellan två punkter i nätet, genom linjär regression av baslinjens avstånd vid de olika epokerna. Resultatet av denna analys är att 7 av totalt 20 baslinjer har sannolikt förändrats (mellan –1,1 och 1,6 mm/år) vid 95 % signifikansnivå. En motsvarande linjär regression av höjdförändringarna visar på små förändringar, men en språngartad ändring av punkt Djup mellan två mätepoker kan inte ges en tillfredsställande förklaring. Vid signifikansnivån 99 % är endast en baslinjeförändring signifikant.

Därefter har hela nätet utjämnats med avseende på punktkoordinater och deras förändringar i tiden ur samtliga observationer (ca 14 miljoner mätningar). Denna analys ger ett alternativt resultat till den enskilda baslinjeanalysen, eftersom alla data hanteras simultant enligt minsta kvadratmetoden. Resultatet av denna utjämning är att tre baslinjer (ingående i de sju, som detekterats ovan) förändras med ca –1 mm/år. Tre punkters positioner i planet relativt punkt Knip (som hållits fast i utjämningen) rör sig 1,2-1,5 mm/år. Dessa rörelser, som alla är statistiskt säkerställda med en risknivå om 5 %, kan eventuellt tyda på små translationer och/eller rotationer längs svaghetszonerna mellan de geologiska blocken, men en sådan tolkning blir vag med föreliggande data. Om risknivån sänks till 1 % rör sig endast punkt Kidr (relativt punkt Knip) signifikant.

Efter denna analys kan man eventuellt dra slutsatsen att målet för studien är uppfyllt, dvs GPS-teknikens lämplighet för studium av små rörelser i jordskorpan i ett mindre område har påvisats. GPS-observationerna är emellertid behäftade med flera systematiska felkällor. Flera av dessa torde vara eliminerade i de skattningar av deformationer som ges av den repeterande mätstrategin. Eftersom jonosfärsaktiviteten tidvis har varit kraftig och hela observationsserien har pågått under en tid då solaktiviteten nått sitt maximum, finns en viss risk att jonosfärsfel påverkat mät- och analysresultaten. (Exempelvis sammanföll mycket kraftiga jonosfärsstörningar med den näst sista mätepoken, med vissa oanvändbara mätningar som följd.) På grund av denna risk borde mätserien fortsätta och helst utsträckas till åtminstone en hel solaktivitetsperiod (ca 11 år). De fortsatta mätningarna kan då eventuellt reduceras från tre till exempelvis två mätepoker/år.

Summary

Since the year 2000 the Swedish Nuclear Fuel and Waste Management Company (SKB) has contracted the Royal Institute of Technology to investigate the feasibility of the space technique offered by the Global Positioning System (GPS) in monitoring possible crustal "creep" in a local geodetic network. For this purpose a geodetic network was established close to Äspö Hard Rock Laboratory, near Oskarshamn in the southeast of Sweden. The network is located in an area of ca 15x20 km, and it is defined by 7 points, later extended by an additional 3 points, consisting of steel markers fixed in drill holes in hard rock. The points were selected at distances of 2–7 km to straddle two geological, possibly active, fault zones. During the GPS observation campaigns each GPS antenna is fixed directly on top of the marker, which therefore must have a good visibility towards the sky all around and down to 10° above the horizon.

By epoch-wise GPS measurements 3 times a year, the goal is to detect any possible crustal deformation of the order of at least 1 mm/yr within a few years. The observations, starting in June 2000, were typically conducted with 7 Trimble 4000 SSE geodetic type GPS receivers, which allow dual frequency phase and code observations. The observation noise level for double difference observations and 15 s integration time is estimated to ca 60 cm and 6 mm for code and phase observable, respectively. In addition, some significant systematic errors, in particular signal multipath and ionosphere bias, may impair the observation quality. In order to minimize data noise and observation site multipath errors, Dorne-Margolin choke ring antennas were used for the satellite signal reception, and observation time was extended to five sessions (days) for each epoch. The ionosphere bias can usually be controlled by the dual frequency observations.

Today, data has been repeatedly collected for almost four years in 11 GPS campaigns. For each epoch campaign, including more than one million observations, the coordinates of the network sites and baseline lengths were determined by a least squares procedure using the Bernese GPS software and by fixing one site in the area. The standard error of the resulting plane and height coordinates are of the order of 1.5-2 mm and 3-4 mm, respectively, and each baseline is determined to ca 1 mm.

By modelling these parameters as functions of time, their temporal changes can be estimated. First, regression analyses were conducted for the epoch-wise results of each baseline estimate, yielding that 7 baselines did not pass the test of no temporal changes at the risk level of 5%. One site moves significantly at the rate of 1.3 mm/yr vs the fixed point of the network.

Second, in a joint data processing of all the data, including ca 14 million observations, the site coordinates and their velocities vs the fixed point were solved simultaneously. As a result, 3 out of 20 dependent baselines change by –0.9, –1.0 and –1.1 mm/yr at a standard error of 0.2-0.3 mm/yr. Site Kidr moves to the SSE at the rate of 1.5 mm/yr, site Stor to the SSV at 1.2 mm/yr, and site Karr moves to the NV at 1.3 mm/yr with respect to a selected fixed point. These motions may indicate that the two blocks rotate counter-clockwise, but this conclusion is not significant based on the present data.

Considering the joint results of the two tests (i.e. regression analysis and simultaneous adjustment of all data) we may conclude that 3 baseline lengths and the horizontal position of site Kidr (vs the fixed site Knip) are verified (at the risk level of 5%) to change of the order of 1 mm/yr. At the risk level of 1% only one baseline (Karr–Kidr) and the position of site Kidr change significantly with time.

No vertical deformations are likely to have been detected. (However, after the third campaign there is a sudden jump of 3 cm at site Djup that cannot be explained.)

From this analysis we may conclude that the goal of the feasibility study has been achieved. Nevertheless, some systematic errors, changing with time, may contaminate the resulting site and baseline velocities. In particular, the ionosphere bias with its eleven-year cycle, reaching a maximum in 2002, may have interfered the results. Extending the study a few more years, possibly to a full cycle of the sun spot activity, which is the driving force of the ionosphere signal variations, can solve this remaining problem.

Contents

1 Introduction

This document reports the results gained by the deformation analysis of the Äspö GPS monitoring network from 2000 to 2004, which is one of the activities performed within the site investigation at Oskarshamn. The work was carried out in accordance with activity plan AP PS 400-02-018. In Table 1-1 controlling documents for performing this activity are listed. Both activity plan and method descriptions are SKB's internal controlling documents.

Table1-1. Controlling documents for the performance of the activity.

Activity plan	**Number**	**Version**
Deformationsmätning med GPS 2003-2004	AP PS 400-02-018	1.0
Method descriptions	**Number**	**Version**
Metodbeskrivning för deformationsmätning med GPS	SKB MD 133.003	1.0

Since several years the Swedish Nuclear Fuel and Waste Management Company (SKB), is investigating various locations for possible long-term disposal of nuclear waste. These various types of site investigations, which will run for many years, will possibly include the monitoring of the stability of the crust by employing the satellite Global Positioning System (GPS) technology. SKB has contracted the Geodesy Group of the Department of Infrastructure, the Royal Institute of Technology (KTH), in Stockholm, to perform a feasibility study by establishing, monitoring and analysing the data of a small deformation network near the Äspö Hard Rock Laboratory at Oskarshamn in the south east of Sweden, Figure 1-1. The goal of the used technique is to admit the detection of possible crustal motions of the order of 1 mm/yr or larger after few years of data collection. After the first period (between 2000 and 2002) of successful GPS measurements of the Äspö deformation network, reported by /Sjöberg et al, 2002/, five more epoch GPS campaigns have been conducted between October 2002 and March 2004. This report evaluates the results of all GPS campaigns in the first and second periods, thus spanning a total time interval of almost four years with 11 epoch GPS campaigns. "

Raw data from the GPS measurements from each campaign has been delivered to SKB. The data reference is listed in Table 1-2.

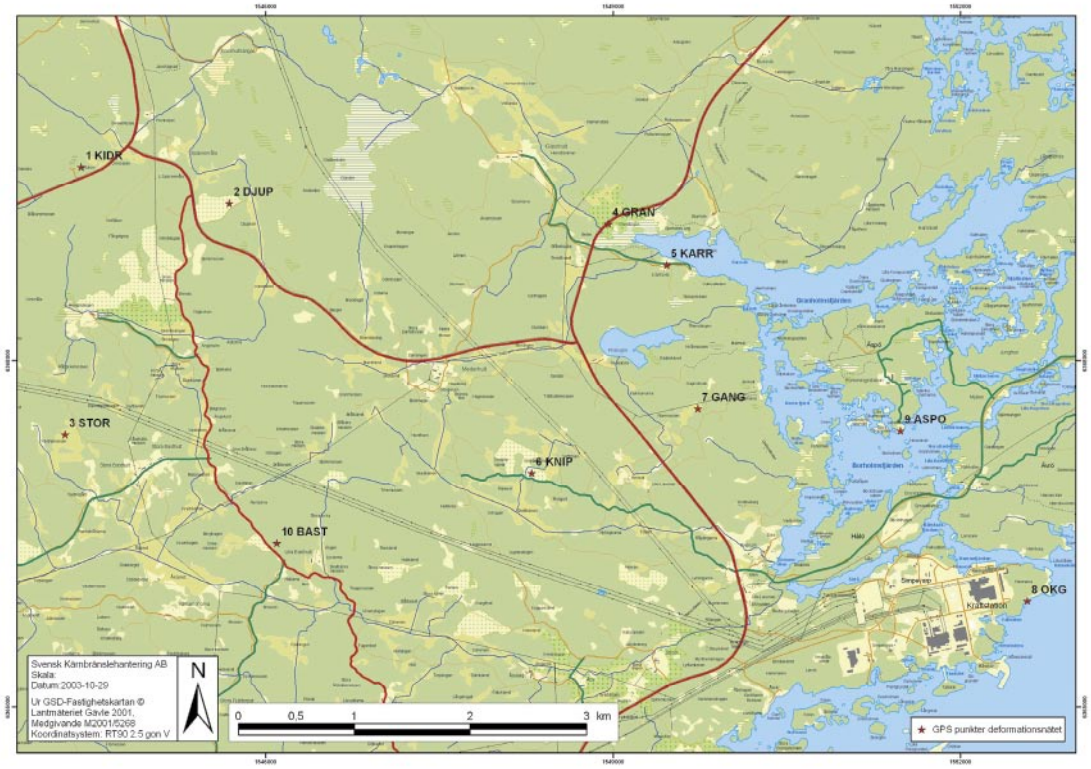

Figure 1-1. *Location of GPS monitoring points in the Äspö local network located within the Oskarshamn investigation site.*

Table 1-2. Data references.

Subactivity	Database	Identity number
Deformationsmätningar under 2000–2003, 2004	SICADA	Field note 156, 229, 300

The names of observation points, corresponding SICADA ID numbers of the observation points and their coordinates in the RT90/RH70 system is listed in Table 1-3.

Table 1-3. Name of GPS observation points, their SICADA ID-number and coordinates in the RT90/RH70 system.

Observation Point	SICADA-ID	Northing X	Easting Y	Elevation Z
1 KIDR	PSM107725	6369668.855	1544413.313	25.714
2 DJUP	PSM107726	6369351.185	1545692.123	18.492
3 STOR	PSM107727	6367359.740	1544272.305	11.697
4 GRAN	PSM107728	6369175.147	1548956.878	9.991
5 KARR	PSM107729	6368828.998	1549463.593	8.216
6 KNIP	PSM107730	6367029.630	1548302.539	20.816
7 GANG	PSM107731	6367581.344	1549730.711	10.951
8 OKG	PSM107734	6365916.408	1552576.487	2.708
9 ASPO	PSM107733	6367393.662	1551480.551	2.011
10 BAST	PSM107732	6366421.711	1546102.760	28.331

2 Objective and scope

SKB is performing site investigations in Oskarshamn. A general program for the site investigations has been published /SKB, 2001a/ as well as a site specific program for the site investigations in Simpevarp /SKB, 2001b/.

In the initial site investigation of the site Oskarshamn deformation measurements with GPS was intented to be used for control of possible slow movements like slip or rotation of rock blocks surrounded by regional deformation zones. Slow movements in the order of 1 mm/yr can be detected after 2–3 years of repeated measurements.

During the year 2000 a feasibility study by using GPS as a tool for detecting slow movements along regional fracture zones was initiated by SKB at seven locations with GPS- receivers and antennas within the Oskarshamn investigation site, Oskarshamn community. The first results from the measurements were presented in a report in 2002 /Sjöberg et al, 2002/.

This activity is a continuation of the method study aiming at the possible detection of slow movements of rock blocks, e.g. slip or rotation, in a local network. More precisely, the aim of the study was to detect any slow movements in the order of 1 to 3 mm/yr with repeated GPS-measurement up to 3 times/yr.

3 The Äspö monitoring network

The original local GPS monitoring network, consisting of 7 sites near Äspö Hard Rock Laboratory in the southeast of Sweden, was established in 2000. It is located across two possibly active faults /SKB, 2000/. In June 2003 the network was enlarged to ten sites (see Figure 3-1). The network is located in an approximate area of 15 × 20 km, spaced about 60 km from the Oskarshamn GPS site of the Swedish permanent GPS network SWEPOS. The distance between two neighbouring sites vary from 2 to 7 km. Each site is defined by a steel benchmark, fixed in the bedrock, for the antenna mount. As the antenna is located only about 10 cm above the ground, the multipath problem, discussed in Section 4-1, may deteriorate the GPS observation. However, efficient multipath protection is warranted by the use of precise choke ring antennas (in comparison to the ordinary Trimble antennas), as this type of antennas are specially designed to minimize the impact of multipath. For all observations Dorne-Margolin type antennas were used. Moreover, at each site bushes and trees in the surrounding were cut down to eliminate all obstacles in any direction of the line-of-sight above the elevation angle of 10°. (However, as the vegetation grows continuously, such obstacles must be removed from time to time.) More detailed information concerning the Äspö network was given in /Sjöberg et al, 2002/. Figures 3-2 to 3-4 show each of the three new stations (Bast, Äspö, and OKG) established in February 2003.

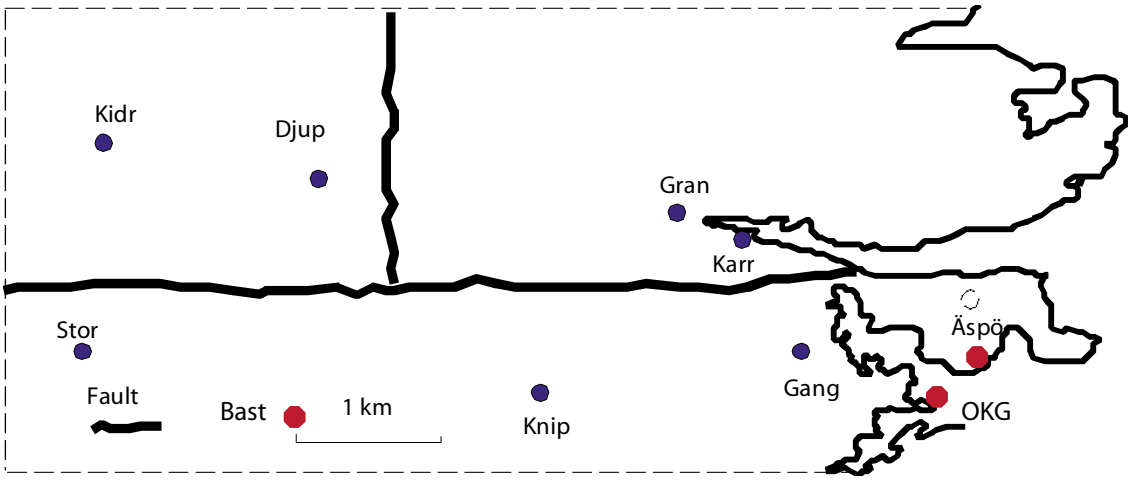

Figure 3-1. *The Äspö GPS monitoring network consisting of ten stations (including the three new stations in red colour) with two possibly active faults.*

Figure 3-2. *A choke ring antenna at site Äspö in March 2004.*

Figure 3-3. *A choke ring antenna with the new type Trimble R7 receiver at site OKG in March 2004.*

Figure 3-4. *A choke ring antenna with a Trimble 4000 SSE GPS receiver at site Bast in June 2003.*

4 Observation errors and their reductions

4.1 GPS observation errors and their reductions

There are a number of error sources in GPS observations. In GPS navigation one uses the C/A code observable with a fundamental wavelength of 300 m. As a rule-of-thumb the noise level is about 1/100 of the wavelength of the signal, which becomes 3 m in the present case. Such a noise would be too imprecise for our application. Instead geodetic GPS receivers use the phases of the 19 and 24 cm carrier wavelengths on L1 and L2, respectively, as the primary observables. This corresponds to a noise level of about 2–3 mm for the raw observable. As explained below, the observable that is used in the final network adjustment is the double difference of phase observations, corresponding to a random error of about 6 mm. In the case of static observations (which applies to our deformation measurements), the noise level is diminished even further in the average by carrying out the observations for at least 48 hours. For the long baseline of ca 60 km between the SWEPOS station at Oskarshamn and the local network the L3 linear combination of the original phase observations L1 and L2 is used to eliminate the ionosphere bias that influences long baselines. However, the L3 observable increases the noise level about three to four times, therefore it is not recommended for short baselines.

The raw phase observation is a function of the distance from the satellite to the observation point. If the satellite positions were known, three such distances, if correctly determined, would be sufficient for intersecting the position of the observer in three-dimensional space (i.e. three observations suffice to determine three coordinates). The low noise discussed above would not greatly harm such a solution, provided that the geometry of the satellites versus the receiver is good.

Unfortunately there are a number of systematic error sources that deteriorates this otherwise excellent observation scheme. These comprise the uncertainties of satellite position and clock, the variable velocity of the signal in the atmosphere, multipath of signal, satellite azimuth and elevation dependent antenna phase centre biases, eccentric position of antenna, hardware delay of signal and receiver clock instability. All GPS softwares utilize standard atmospheric models to estimate the signal delay in the ionosphere and troposphere. A standard trick to reduce (or even eliminate some) error sources is to take differences between the simultaneous observations from two GPS receivers and two satellites, which observable is called a double difference. This concerns the clock errors, satellite positions and atmospheric errors.

For some of these systematic errors, such as the errors caused by the atmosphere, the systematic error reduction by this difference observable is dependent on the baseline length between the receivers. Most annoying for baselines longer than, say, 15 km is the signal delay caused by the ionosphere. (For the most precise applications the ionosphere effect might be significant also for shorter ranges.) As already mentioned the ionosphere bias can be eliminated by the so-called ionosphere-free linear combination (L3) of the L1 and L2 phase observations at the price of 3.6 times increased noise level. For shorter baselines it must therefore be judged if the use of L3 is worth this price. The ionosphere activity is strongly correlated with the sunspot activity, and the solar activity may be characterised by an 11-year cycle. The last ionosphere maximum (prior to this study) occurred in 1989/1990, and the ionosphere activity was rather strong during our observation campaigns, reaching

a new maximum in 2002 as was expected (see Figure 4-1 below). The figure shows the mean Total Electron Content (TEC) that has been abstracted from the global ionosphere maps produced by the International GPS Service /IGS; Schaer, 1998/. This parameter roughly describes the ionospheric activity on global scale. As solar activity increased in 2002, the ionosphere bias increase and became more variable and therefore harder to model and predict. Irregularities in the ionosphere produce short-term signal variations. These scintillation effects may cause a large number of cycle slips of the satellite signal, because the GPS receiver cannot record the short-term signal variations. Also, high electron contents can produce strong horizontal gradients, which corrupt the phase ambiguity solution. Some details on the actual ionosphere conditions during the observation period 2000–2004 are given in Section 4.2.

The positions of the GPS satellites are nowadays very well computed by IGS, which provides orbital information to the user.

Multipath is reduced if the observation site is selected with care in an open space without reflecting surfaces in the surrounding. Also, the most advanced choke-ring antennas efficiently reduce multipath.

Antenna phase centre variations, of the order of a few millimetres, can be controlled by an individual calibration of each antenna. For precise deformation analyses it is important that the error caused by an eccentric positioning of the antenna is eliminated by so-called forced centring. Also, by using the same antenna with the same orientation at each set-up at a point some antenna biases are avoided.

The carrier phase observations cannot be fully explored unless the integer phase ambiguities (i.e. the numbers of full cycles of the satellite-to-receiver ranges) have been determined (i.e. fixed to integer values). Noisy and biased data will inevitably impair the possibility to fix the ambiguities, and if caution is not taken, the wrong ambiguities might be fixed. As the carrier wavelength is about 20 cm, each erroneous cycle corresponds to an erroneous satellite-to-receiver observation of this magnitude. For precise GPS positioning it is therefore a necessity to reliably fix the integer ambiguities. However, in the case of static observations for sessions of several hours of duration with baselines not exceeding, say, 15 km and good observation conditions, there should be no problem to meet these demands.

4.2 The ionosphere activity 2000–2004

Figure 4-1 shows the variation of the total electron content of the ionosphere along a line of sight from 1995 to 2004 with a prediction to 2005. This variation is related with the 11–year solar activity, having a maximum in 2001/2002. In addition there are daily variations as can be seen from Figures 4-2 and 4-3.

The electron content of the ionosphere delays the GPS signal, leading to a biased satellite-to-receiver range estimate when using the basic L1 and L2 observables. If the ionosphere delay were not modelled at all, single point positioning by GPS would suffer from a satellite-to-receiver range bias of the order of 10 m. Normally this bias cancels in a short baseline estimation by GPS, while the error is more pronounced in long baselines (say, for baselines exceeding 15–20 km). For this reason, the L3 ionosphere-free linear combination of L1 and L2 is advantageous for long baselines, although it has the bad property of increasing the noise level compared to the basic signals, making it less advantageous

for short baselines. However, for extreme requirements and extreme ionosphere activity, the bias might be significant also for small baselines. This fact will be considered in the analysis that follows in Chapter 7 and later.

For short baselines L1 will be used as the primary observable together with a global ionosphere model determined by the L1 and L2 observations, see Chapter 6.

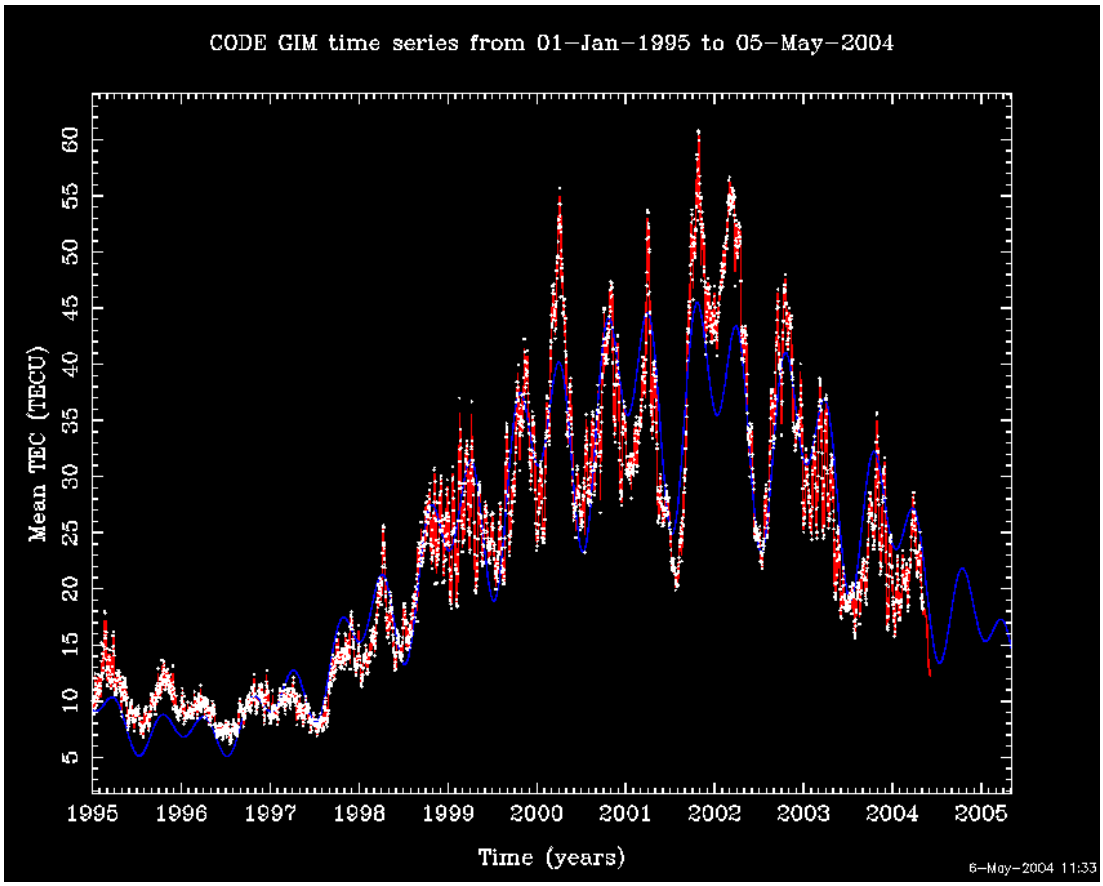

Figure 4-1. *The ionosphere activity in units of Total Electron Content (TEC) for the period 1995–2004 (from International GPS Service). Note: red line represents the real ionosphere activity and blue line is the predicted activity. 1TEC =10^{16} electrons per m^2.*

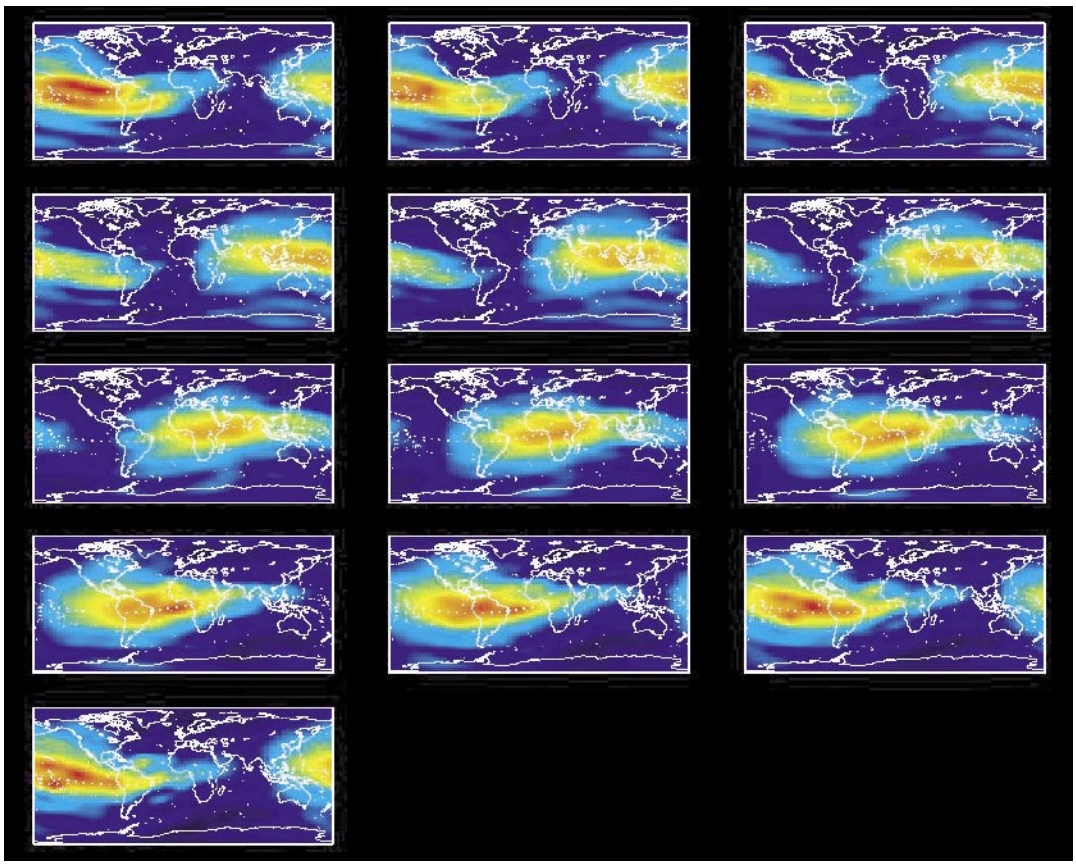

Figure 4-2. *2-hourly global Total Electron Content (TEC) snapshots for February 16, 2004, as produced by IGS.*

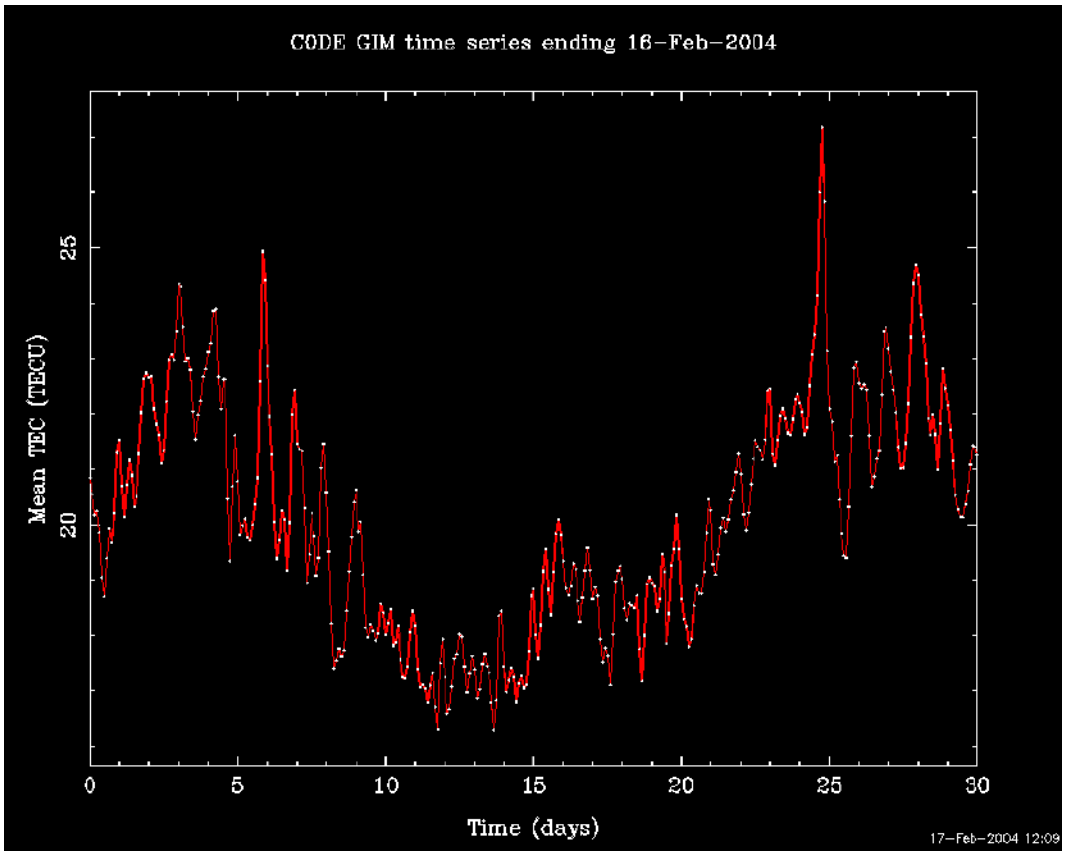

Figure 4-3. *One month of mean Total Electron Content (TEC) retrievals ending 16th February 2004. (From IGS.)*

5 Execution

5.1 Results of the epoch campaigns from 2000 to 2002

As reported in /Sjöberg et al, 2002/, six GPS campaigns were carried out between the years 2000 and 2002, each for three days, namely 27–29 of June and 26–28 of September in 2000, 16–18 of January 12–16 of June and 16–19 of October in 2001 and 20–22 February in 2002. The GPS data have been processed with the Bernese GPS software Version 4.2. The principal results of the data analysis are the site and baseline velocities, being computed in the program ADDNEQ. The formal/internal precision of the velocity estimation of the adjustment of all campaigns by the ADDNEQ is too optimistic due to the fact such the software neglects the existing temporal correlations among the huge number of GPS data. The standard errors and error-ellipses have therefore been scaled up by a factor 7–10 to represent approximately the external precision from all the campaigns /Becker et al, 2000; Fridez, 2002/.

As expected, the result of only two years of data collection and analysis could not detect any crustal motions, but the bedrock in the investigation area seems very stable. Only the estimated motion at site Kidr was significant at the confidence level of 95%. The previous theoretical calculation showed that if the accuracy of the epoch-wise estimated horizontal coordinate or baseline length is about 1.5 mm, which is reasonable for our GPS data and analysis, it takes 3 years to detect a deformation at the rate of 1 mm/yr or more. The same order of a vertical rate of motion will take 5 years to detect due to worse quality of such data. These estimates do not consider possible systematic errors in the data. Unfortunately, we know that the solar activity, with increased ionosphere GPS signal delay and disturbance, has been rather high during the observation period, and its development during the next few years is also bad (see Section 4.2). The ionosphere activity is likely to make the GPS signal noisier, but, more severe, possible non-modelled ionosphere biases may significantly influence the result of the analysis as well.

5.2 GPS campaigns from October 2002 to March 2004

The six old epoch campaigns, conducted between 2000 and 2002, were described in /Sjöberg et al, 2002/ and summarized in Section 5.1. The new GPS data, to be added in this analysis, were collected during 5 new epoch GPS campaigns (including data from the SWEPOS station at Oskarhamn) from October 2002 to March 2004. This section describes these new (7th to 11th) GPS observation campaigns.

Five GPS campaigns were carried out in this second period of observations, each for four or five days, namely from October 29 to November 2 in 2002, February 23–25, June 24–28, and from October 28 to November 1 in 2003 and between March 16 and 20, 2004. At each site the data was recorded at 15-second intervals for a total of 50 hours with Trimble 4000 SSE GPS receivers. The three new stations (Bast, OKG, and Äspö) were added to the network in June 2003 (see Figure 3-1). As there are only the seven Trimble receivers available, the extended network had to be measured in two additional sessions: after 50 hours of observations three receivers were moved from stations Stor, Kidr and Gran to the new sites Bast, OKG and Äspö, and the remaining sites Djup, Karr, Gang, and Knip were continuously measuring with the original receivers. Unfortunately, the memory capacities of the receivers are not sufficient to record the data of a full session, but the data

had to be transferred from the receivers to personal field computers after ca eight hours of measurements, which means that each receiver had to be emptied twice a day (morning and evening) (see Figure 5-1).

In order to avoid antenna location biases the series number of each choke ring antenna was recorded at each site. In this way it would be possible to use identical antennas at each site for all campaigns. Unfortunately, KTH did not have its own set of antennas until very recently, so antennas had to be borrowed for most campaigns. As a result, it was not always possible to get the same set of antennas to be repeatedly used at each site. It is therefore possible that this problem may have caused some biases in the data.

Surface measurements of temperature, pressure and relative humidity were not recorded during the campaigns, as our long experience has proved that such information does not improve the results.

5.2.1 The 7th campaign

The 7th GPS campaign of the local GPS network was performed from October 29 to November 2, 2002. The sites were occupied by seven Trimble 4000 SSE receivers and Dorne-Margolin type choke ring antennas. Two receivers, with outdated internal software, were borrowed from the community of Stockholm. The old software could affect the accuracy of measurements. To sort out this problem, we replaced the two receivers (numbers S/N 2283 and S/N 2357) by two other receivers (numbers S/N 6243 and S/N 4870) with the updated software after about 48 hours of observation. The total occupation time was about 96 hours on each station. The observation windows and the receiver/antenna pairs used for the measurements are given in Table 5-1.

Figure 5-1. *A personal field computer was transferring GPS data from a Trimble 4000 SSE receiver.*

Table 5-1. Observation time and receiver/antenna pairs used in the 7th campaign. Note *: Receiver S/N 4870 was changed to receiver S/N 2283 after 48 hours of observation.

Station	Observation time	Receiver S/N	Antenna S/N	Status of GPS data
Knip	9:00 Oct. 29 to 12:00 Nov. 02 2002	10054	1998380117	OK
Kidr	9:00 Oct. 29 to 11:00 Nov. 02 2002	4870 to 2283*	11934	OK
Stor	9:00 Oct. 29 to 11:30 Nov. 02 2002	4880	3231A01229	OK
Djup	9:00 Oct. 29 to 11:40 Nov. 02 2002	2283 to 4870*	620011003	OK
Karr	9:00 Oct. 29 to 11:50 Nov. 02 2002	2357 to 6243*	6200327020	OK
Gran	9:00 Oct. 29 to 12:30 Nov. 02 2002	6243 to 2357*	6200327024	OK
Gang	9:00 Oct. 29 to 12:40 Nov. 02 2002	6246	6200327021	OK

5.2.2 The 8th campaign

The 8th measurement campaign was performed between February 23 and 25, 2003. The observation time was about 70 hours. (During this time the three new stations (Bast, OKG, and Äspö) were constructed, to be ready to take part in future campaigns.) The observation windows and the receiver/antenna pairs used for the measurement are given in Table 5-2.

Table 5-2. Observation time and receiver/antenna pairs used in the 8th campaign.

Station	Observation time	Receiver S/N	Antenna S/N	Status of GPS data
Knip	9:00 23 to12:00 Feb.25 2003	10054	199880114	OK
Kidr	9:00 23 to11:20 Feb.25 2003	6614	15603	OK
Stor	9:00 23 to11:00 Feb.25 2003	1229	15600	OK
Djup	9:00 23 to11:30 Feb.25 2003	2357	251	OK
Karr	9:00 23 to11:40 Feb.25 2003	4870	11934	OK
Gran	9:00 23 to12:20 Feb.25 2003	4880	199880117	OK
Gang	9:00 23 to 12:30 Feb.25 2003	6613	14256	OK

5.2.3 The 9th campaign

The 9th measurements were performed in June 24–28, 2003. As before, seven receivers and antennas were used for this campaign. Three of the receivers and antennas at stations Stor, Kidr and Gran were moved to stations Bast, Äspö and OKG after about 48 hours of observation (see Table 5-3), while the rest were kept measuring to the end of the campaign. At one event the receiver at site Karr slipped down on the rock, possibly caused by an animal. Fortunately, the cables were still connected and data was not lost (See Figure 5-2). The observation windows and the receiver/antenna pairs used for the measurements are given in Table 5-3.

Table 5-3. Observation time and receiver/antenna pairs used in the 9th campaign.

Station	Observation time	Receiver S/N	Antenna S/N	Status of GPS data
Knip	9:00 24 to 12:00 June 28 2003	6613	1998380115	OK
Kidr	9:20 24 to 10:00 June 26 2003	2283	1998380117	OK
Stor	9:30 24 to 10:30 June 26 2003	1229	239	OK
Djup	9:40 24 to 12:30 June 28 2003	2357	15600	OK
Karr	10:20 24 to 13:00 June 28 2003	4870	11934	OK
Gran	10:30 24 to 11:00 June 26 2003	4880	15603	OK
Gang	12:00 24 to 11:40 June 28 2003	6614	14256	OK
Bast	11:00 26 to 13:00 28 2003	1229	239	OK
OKG	11:20 26 to 12:40 28 2003	4880	15603	OK
Äspö	11:00 26 to 13:30 28 2003	2283	1998380115	OK

5.2.4 The 10th campaign

The 10th measurements were performed from October 28 to November 1 in 2003. Now seven new Dorne-Margolin type choke ring antennas had been purchased by KTH, simplifying the planning of future campaigns to allow identical antennas be set up at each station and campaign. Three of these receivers and antennas at stations (Stor, Kidr and Gran) were moved to stations (Bast, Äspö and OKG) after about 48 hours of observation, while the rest were kept measuring to the end of the measurement campaign. The observation windows and the receiver/antenna pairs used for the measurement are given in Table 5-4. At this campaign, after three years of use, some car batteries were not functioning well. This caused some minor problems, including that site Karr lost power for about 4 hours.

Table 5-4. Observation time and receiver/antenna pairs used in the 10th campaign.

Station	Observation time	Receiver S/N	Antenna S/N	Status of GPS data
Knip	9:00 Oct. 28 to 11:20 Nov.1 2003	2357	6200327016	OK
Kidr	9:20 Oct. 28 to 10:00 Nov.30 2003	6614	5200327001	OK
Stor	9:30 Oct. 28 to 10:30 Nov.30 2003	1229	6200327023	OK
Djup	10:00 Oct. 28 to 11:30 Nov.1 2003	2283	6200327017	OK
Karr	10:30 Oct. 28 to 12:00 Nov.1 2003	10054	6200327020	OK
Gran	11:00 Oct.28 to 12:00 Oct.30 2003	4880	6200327024	OK
Gang	11:30 Oct. 28 to 12:20 Nov. 1 2003	4870	6200327021	OK
Bast	11:00 Oct. 30 to 12:30 Nov.1 2003	1229	6200327023	OK
OKG	12:20 Oct. 30 to 12:40 Nov. 1 2003	4880	6200327024	OK
Äspö	11:00 Oct. 30 to 12:00 Nov. 1 2003	6614	5200327001	OK

During this observation campaign strong solar activities were recorded. The satellite installed Solar and Heliospheric Observatory, launched on December 1995, with a Large Angle Spectrometric Coronagraph and the Extreme Ultraviolet Imaging Telescope instruments, was provided with an unprecedented opportunity for continuous real-time monitoring of solar eruptions. The observatory observed that an enormous solar prominence, 30 times the size of the earth, erupted from the Sun on October 28 /Brekke, 2003/ (see Figures 5-3 and 5-4). The sun activity has direct effects on various topics such as communication systems, aircrafts, radar and GPS systems, etc. This time the sunspot activity was so strong that it destroyed some electric systems at Malmö region in the south of Sweden and thousands of houses were without electricity for several hours. For security reasons it was decided to lower the temperature of the nuclear generators at Oskarshamn. Unfortunately, this sun spot activity overlapped with the 10th GPS campaign, and it therefore corrupted some of the data (see Section 7.1).

Figure 5-2. *The receiver at site Karr slipped down from the box to the rock in June 2003. Fortunately, the cables were still connected and data was not lost.*

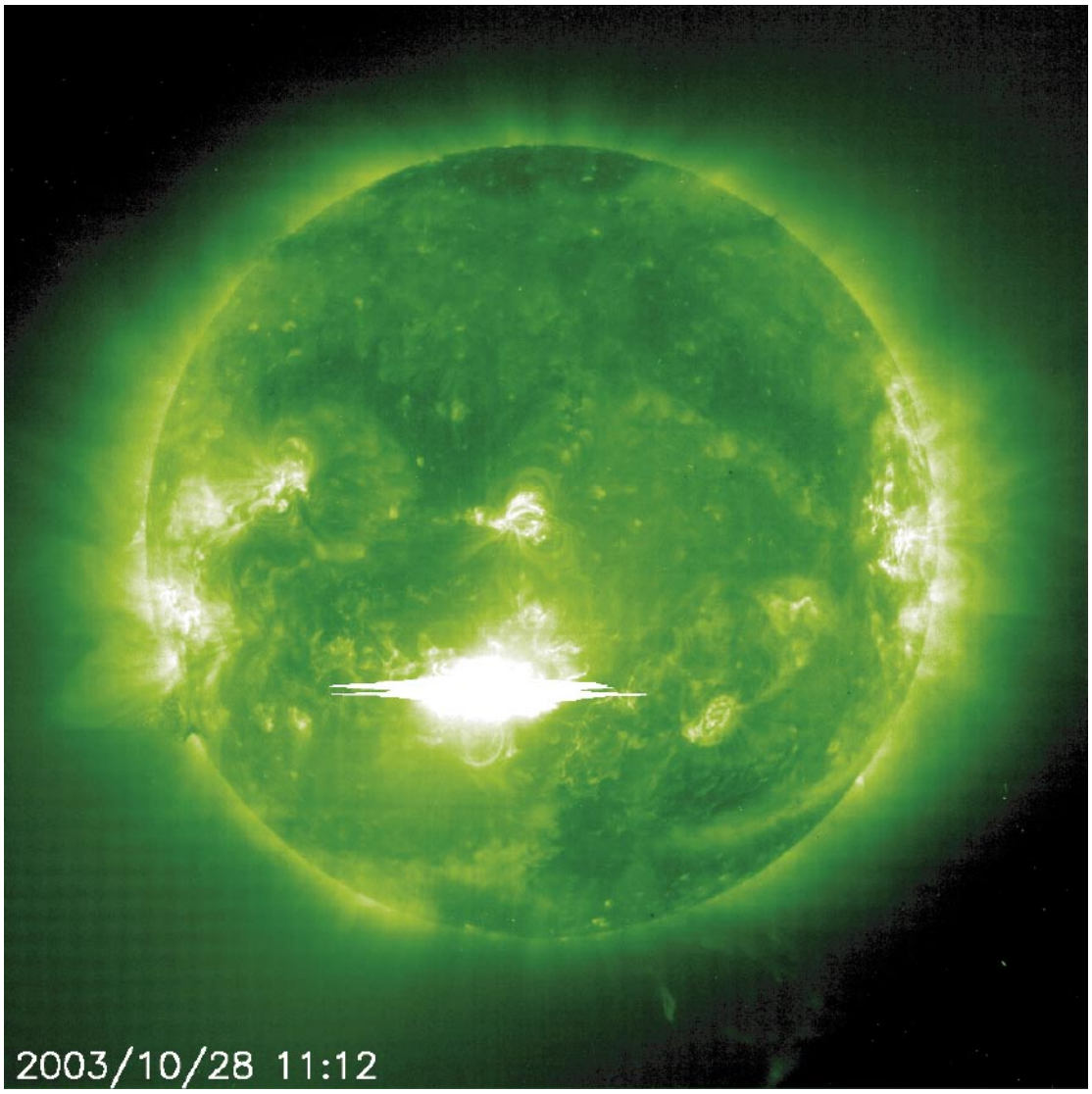

Figure 5-3. *The biggest solar X-ray flare ever recorded saturated the X-ray erupted detectors on several monitoring satellites. It has been classified as an X28 flare. The associated coronal mass ejection came out from the Sun's surface at about 2,300 km per second (8.2 million km/h) on October 28 (from the Solar and Heliospheric Observatory). Unfortunately, the fourth GPS campaign (from October 28 to November 1 in 2003) coincided with the time of the enormous solar activity, which affected accuracy of the GPS measurements without suspect.*

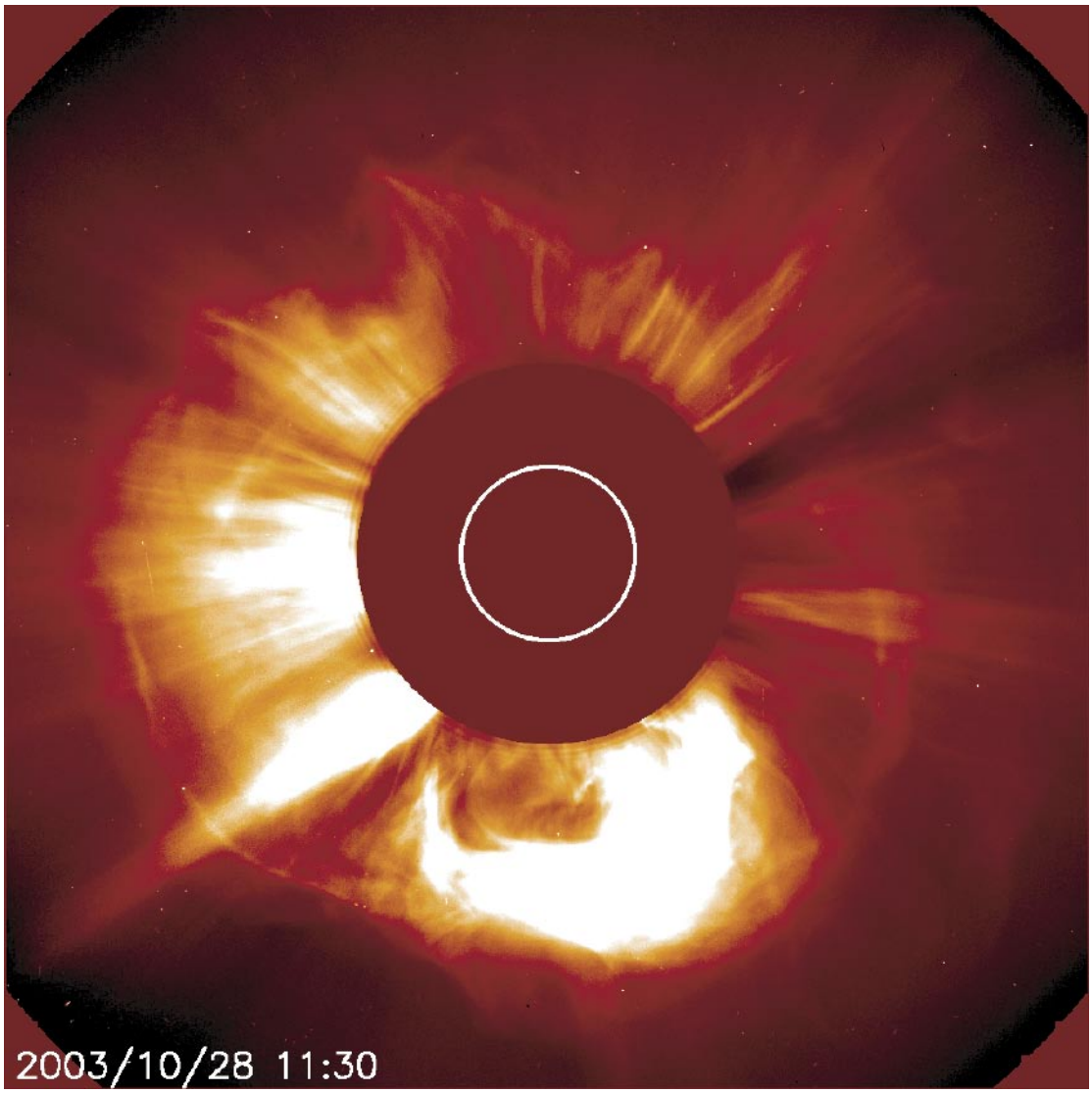

Figure 5-4. *An enormous solar prominence, 30 times of the size of the earth, erupted from the Sun on October 28 (from the Solar and Heliospheric Observatory). Unfortunately, the fourth GPS campaign (from October28 to November1 in 2003) coincided with the time of the enormous solar activity, which affected accuracy of the GPS measurements without suspect.*

5.2.5 The 11th campaign

The 11th set of measurements was performed in March 16–20, 2004. Three Trimble R7 receivers of the new type were tentatively compared with the old Trimble 4000 SSE receivers. Hence three Trimble R7 receivers, 7 Trimble 4000 SSE and nine choke ring antennas were used. Unfortunately, an old Trimble 4000 SSE receiver at site Djup was damaged at the beginning of the observation session, and one unit of the new type R7 receiver was used instead (see Figure 5-5). After 48 hours of observation the Trimble receiver at site Karr was moved to the site Djup. Three of these receivers and antennas at stations Stor, Kidr and Gran were moved to stations Bast, Äspö and OKG after about 48 hours of observation in a planned way, while the rest of two receivers were kept measuring to the end of the campaign. The three new R7 receivers were installed for about 48 hours at stations Djup, Kidr, OKG, Bast and Stor. The observation windows and the receiver/antenna pairs used for the measurement are given in Table 5-5.

Table 5-5. Observation time and receiver/antenna pairs used in the 11th campaign. Note: * means that receiver or antenna was replaced.

Station	Observation time	Receiver S/N	Antenna S/N	Status of GPS data
Knip	9:00 16 to 11:00 Mar. 20 2004	2357	6200327016	OK
Kidr	9:20 16 to 10:00 Mar.20 2004	6614 to R7 0220325987*	5200327001 to15603*	OK
Stor	9:30 16 to 10:30 Mar.20 2004	1229 to R7 0220325986*	6200327023 to15600*	OK
Djup	10:00 16 to 11:30 Mar.20 2004	R7 0220325970 to 10054*	6200327017	OK
Karr	10:30 16 to12:00 Mar.20 2004	10054 to R7 0220325970	6200327020	OK
Gran	11:00 16 to 12:00 Mar.18 2004	4880	6200327024	OK
Gang	11:30 16 to 12:20 Mar. 20 2004	4870	6200327021	OK
Bast	11:00 16 to 12:30 Mar.20 2004	R7 0220325986 to 1229*	15600 to 6200327023*	OK
OKG	12:20 16 to 12:40 Mar. 20 2004	R7 0220325987 to 4880*	15603 to 6200327024*	OK
Äspö	11:00 18 to 13:00 Mar. 20 2004	6614	5200327001	OK

Figure 5-5. *A new Trimble R7 receiver being tested at site Djup in March 2004.*

5.3 The SWEPOS station at Oskarshamn

In order to use precise satellite orbits and their related coordinate systems provided by the International GPS Geodynamics Service (IGS), the local Äspö network has to be connected to the global GPS network by the Swedish network of permanent reference stations (SWEPOS). In 1991 the National Land Survey of Sweden, in co-operation with Onsala Space Observatory, Chalmers University of Technology, started to build up the SWEPOS network /Hedling and Jonsson, 1995/. The first six test stations were successfully operating in 1992, and today the continuously operating network consists of 25 SWEPOS stations unified throughout Sweden. The major application includes geophysical research (measuring three-dimensional crustal deformation rates of continental scale with sub-mm per year resolution) as well as a contribution to a new geodetic infrastructure (i.e. the establishment and maintenance of a reference system) of global, Nordic and national scale, and a rapid positioning service in real-time for surveying and navigation with an accuracy of about 1 m, as well as the CICERON service, which provides cm accuracy.

The nearest SWEPOS station, Oskarshamn (see Figure 5-6), close to the Äspö network, was used in our GPS processing in order to get excellent a priori co-ordinates in the International Terrestrial Reference Frame (ITRF). The Terrestrial Frame Section of International Earth Rotation Service is in charge of producing and maintaining the ITR System (ITRS). The coordinates and their velocities of the ITRF reference stations have primarily been determined by precise space geodetic techniques, such as Very Long Base Interferometry, Satellite Laser Ranging, Lunar Laser Ranging and GPS, to optimise the realisation of the ITRS, which is then called the ITRF /Sillard and Boucher, 2001/. The working reference system of an individual analysis is generally conventionally defined in such a system. In this way the motion of the Äspö network can be analysed relative to the SWEPOS station at Oskarshamn.

Figure 5-6. *The SWEPOS station Oskarshamn with a choke ring antenna (with courtesy from SWEPOS).*

6 Description of the GPS processing method

For standard applications, GPS observations are usually processed using software provided by the receiver vendors, occasionally developed by specialized software suppliers, usually optimised for convenience and ease of use. For example, the software GPSurvey is used for the Trimble GPS receiver. Such a kind of software is easy to use as a "black box", making already slightly trained personnel quickly productive. The black box is not suitable for our scientific research, where the utmost of the GPS signal-to-noise ratio is needed for a successful analysis.

Instead the Bernese GPS software Version 4.2 /Hugentobler et al, 2001/ was used in processing the observation data. The Bernese software is one of a number of scientific GPS software packages, such as Gamit, that is provided with the source code. The user is even required to compile the program from the source. Bernese, like Unix, is user-friendly, but it needs to be used with great care. The user interface consists of a series of text screens operated strictly through the keyboard. Although the manual consists of 500 pages, it still is not complete. The software is a complex system, which models a great number of physical effects that are relevant not only to the measurement process, but also to the behaviour of the GPS satellites as celestial bodies among the natural planets of the Earth and that of the Earth as a dynamic planet in space. Physical models used in the software include:

- Orbital motion of the GPS satellites, including non-inertial forces such as radiation pressure.
- Effects of other celestial bodies, like Sun, Moon and greater planets.
- The effect of the attitude of the GPS satellites on the measurements.
- The behaviour of GPS clocks.
- Earth rotation parameters like polar motion and length of day.
- Earth tides, ocean tides and the elastic response of the solid Earth to these.
- The effects of antenna type on error propagation.
- The propagation effects of ionosphere and neutral atmosphere.
- Finally, (what is not strictly a physical phenomenon) choice of reference frame for the computations and coordinate frame transformations.

The chosen strategy for GPS observation is epoch-wise campaigns. Primarily, the GPS observations of the Äspö GPS network are processed epoch by epoch. As the network at the end of the study period consists of ten sites about 5 km apart within an area of 15×20 km approximate size, and the SWEPOS station Oskarshamn is about 60 km away from the network, two different methods were used for the computations, namely the standard techniques for short or long baselines, respectively. This means that the long baseline from Oskarshamn to a selected GPS station in the local network (Knip) was adjusted as a long baseline, while the local network was adjusted by the technique for short baselines. Major guidelines on how we dealt with the data are briefly described below:

- First, the coordinates of station Knip was determined by adjusting the observations from the long baseline Oskarshamn to Knip by keeping Oskarshamn fixed to its ITRF97 /Boucher et al, 1999/ coordinates provided by SWEPOS. The primary measurement was the L3 ionosphere-free linear combination dual frequency phase observable.

- Second, station Knip was kept fixed for the Äspö network, and daily solutions were processed using L1 phase observations /Hugentobler et al, 2001/.
- Apply Ocean Loading Corrections.
- Use 10° elevation cut off angle and apply elevation dependent weighting.
- All available observations were recorded at 15-sec observation rate.
- Correlations between the baselines were correctly modelled.
- No a priori troposphere model is used, but the total zenith path delays are estimated by the Dry Niell Mapping function /Hugentobler et al, 2001/. The troposphere zenith delays were estimated together with the other parameters. One absolute and three relative parameters, both with an a priori accuracy of 5 cm, were included per station and session for each campaign. Estimation of tropospheric zenith path delays was carried out in 6-hour intervals for the network and 4 hours intervals for the Knip–Oskarshamn baseline.
- The "geometry-free" linear phase combination

$$L_4 = L_1 - L_2 \qquad (1)$$

was used for the estimation of a regional ionosphere model. (Notice that L_4 is independent of receiver clocks and geometry (orbits, station coordinates; /Rothacher et al, 1996/). It only contains the ionosphere delay and the initial phase ambiguity.) From the L_4 observations the following observation equations were selected (Equation (13.9a) of /Hugentobler et al, 2001/):

$$L_4 = -a\left(\frac{1}{f_1^2} - \frac{1}{f_2^2}\right) F_1(z) E(\beta, s) + B_4, \qquad (2)$$

where L_4 is in units of metres, a is a constant, f_1 and f_2 are the frequencies of the carriers L_1 and L_2, $F_1(z)$ is a mapping function (considered as known) evaluated at the zenith distance z, B_4 is a constant bias and $E(\beta s)$ is the vertical Total Electron Content (TEC) represented as a function of geographic or geomagnetic latitude β and sun-fixed longitudes (see below).

The regional TEC model, that was applied in the vicinity of one or more dual-frequency GPS stations, was represented by the power series (Equation (13.10) of /Hugentobler et al, 2001/):

$$E(\beta, s) = \sum_{n=0}^{n_{max}} \sum_{m=0}^{m_{max}} E_{nm} (\beta - \beta_0)^n (\lambda - \lambda_0)^m, \qquad (3)$$

where n_{max} and m_{max} are the maximum degrees of the two-dimensional Taylor series expansion in latitude β and longitude λ, respectively, β_0 and λ_0 are the coordinates of the origin of the development, and E_{nm} are the unknown TEC coefficients of the Taylor series to be estimated in the local model. For example, on 18th January 2001 a regional ionosphere model was estimated for the Äspö network with n_{max} and m_{max} set to 1 with the following result:

$E_{00} = 1.0598 \pm 0.0061$ $\quad$ $E_{01} = 0.3357 \pm 0.0017$

$E_{10} = -0.3511 \pm 0.0026$ $\quad$ $E_{11} = -0.0495 \pm 0.0013$.

Once the unknown parameters of Equations (2) and (3) have been computed by the least squares method, the ionosphere delay $\delta\rho^i_{ion}$ for the observation carrier L_i (i = 1, 2) can be estimated by the formula /Spilker, 1978/:

$$\delta\rho^i_{ion} = -4\, E(\beta,s)/(f_i \cos Z), \qquad (4)$$

where Z is zenith distance at the so-called ionosphere point.

- Precise GPS satellite ephemerides were used, offered by IGS in the ITRF97 system for the 2000 and 2001 campaigns, but from 2002 ITRF00 was offered by IGS. The precise orbits of the last campaign were transferred from ITRF00 to ITRF97 at the observation epoch using a seven-parameter Helmert transformation.
- The integer phase ambiguities were resolved independently on L1 and L2 phase observations using the SIGMA algorithm for short baselines, and for the long baselines from Oskarshamn to the network the Quasi ionosphere-Free (QIF) strategy was used.
- The data was processed session by session (or day by day), and normal equations (NEQ) of all the sessions were stored. Then, the results were combined to obtain final solutions of the campaign, using the combination program ADDNEQ and calculating repeatablities of estimated coordinates as internal accuracy of the campaigns.
- No a priori troposphere model was used for troposphere correction, instead of Dry Niell Mapping function /Hugentobler et al, 2001/. The troposphere zenith delays were estimated together with the other parameters. One absolute and three relative parameters, both with an a priori accuracy of 5 cm, were included per station and session for each campaign. Estimation of tropospheric zenith path delays was carried out in 6-hour intervals for the network and 4 hours intervals for the Knip–Oskarshamn baseline.

In order to save computer time, the normal equations of each session were stored. Then, all sessions were combined to get a final campaign solution. This was done in the program ADDNEQ. In addition to the above-described parameters, the previously fixed parameters could be estimated as well. The program ADDNEQ only uses the stored normal equations without taking care of the original observations. This program may simplify and considerably accelerate the calculations without loss of any information.

7 Processing the GPS observations

One of the main principles of the GPS processing is to eliminate the ionosphere bias by using the dual frequency observations L1 and L2. This is possible by the L3 combination of the L1 and L2 observations. However, it is well known that while the L3 combination eliminates the ionosphere bias, it has the disadvantage to increase the noise of the observable three times relative to the L1 observable alone. As the ionosphere bias increases with baseline length, the L3 observable is advantageous for long baselines, where the ionosphere bias dominates the error sources, while the L1 observable, combined with a simple ionosphere model, is usually more advantageous for a network consisting of short baselines. This standard scheme may have been somewhat disturbed by the fact that most of our GPS campaigns were conducted during increased solar activities. For this reason, the two observation types will be compared in our analysis.

Another important processing feature is to estimate the troposphere delay parameters. In small areas with little height variation it is possible to assume that the thickness of the neutral atmosphere is constant and thus nearly the same above the end points of every baseline vector. One troposphere zenith delay (TZD) parameter was chosen to correct the troposphere delay for each station. Such a parameter describes the total along line of sight signal delay as TZD/cos z, where the cosine describes the geometric path lengthening with increasing zenith distance angle z. When estimating TZD parameters in a small area, no a priori troposphere model was used for troposphere correction, but the Dry Niell Mapping function /see Hugentobler et al, 2002/ was directly estimated in the least squares adjustment stage. Hence, the troposphere zenith delays were estimated together with all other parameters, which are time dependent for long sessions.

In processing the GPS carrier phase observation data, the coordinates of one station usually has to be fixed as known in the ITRF system (as precise orbits were used in ITRF system from the International GPS Geodynamics Service). Large deviations of the coordinates from their true values may introduce errors to the calculated baseline components. The coordinates of the fixed station are obtained from single point positioning with an accuracy of several metres, which is not sufficient for the analysis of deformations. Fortunately, one way out of this issue to connect the fixed station to a reference station (Oskarshamn) controlled by SWEPOS. The coordinates of the Oskarshamn station are listed in Table 7-1 in the ITRF96 system offered by SWEPOS. As the precise ephemerides were used, offered by (IGS) in the ITRF97 system, the coordinates of the Oskarshamn station were transferred from ITRF96 to ITRF97 at the observation epoch using a seven-parameter transformation. As the IGS precise orbits after 2002 were used in ITRF00 system, the orbits were transferred back to ITRF97 from ITRF00.

Table 7-1. The coordinates of the reference station Oskarshamn at the epoch 1999.3 in the ITRF96 system offered by SWEPOS.

Station	X(m)	Y(m)	Z(m)
Oskarshamn	3341339.982	957912.421	5330003.341

The data were processed as day-by-day sessions, and normal equations (NEQ) of all the sessions were stored. After that, the results were combined to a final solution of each campaign, using the combination program ADDNEQ.

As the baseline lengths of the network are only about 5 km, except for the baseline from Oskarshamn to the rest of the network (about 60 km), in general about 95% of the integer phase ambiguities were resolved. Some ambiguities could not be resolved due to the fact that those satellite signals were interrupted by trees, multipath, or severe ionosphere activity.

7.1 Internal precision of the campaigns from 2002 to 2004

The standard error of unit weight of a GPS network adjustment is a measure of precision, i.e. a measure of the fit of the data to the used model for the adjustment. If there is no absolute control or conditions included in the adjustment, the standard error of unit weight is frequently a rather bad measure of the accuracy of the network. This fact is related with that systematic errors are frequently hidden and not reflected in the standard error. A better way to assess the quality of the overall solution is to estimate the coordinate repeatability, which shows an internal consistency that can better reflect the real GPS accuracy compared to the standard errors obtained directly in the network adjustments. (However, also now some systematic errors could be masked, yielding a too optimistic quality estimate.)

The repeatability measure of an observation campaign is defined as the Root Mean Square (RMS) value of the daily coordinate solutions vs the mean values of the total campaign. The repeatabilities, in units of mm and in the local north-east-up coordinate system, are listed in Tables 7-2 to 7-6 for all the five campaigns between 2002 and 2004, respectively, with station Knip being fixed. These tables, based on the adjustment of the L1 observable, show that the horizontal precisions are about 1 mm with a maximum of 3.0 mm for site Bast in the June 2003, Table 7-4 (with an exception in October 2003, Table 7-5; see below). Vertical precisions are about 3 mm with a maximum of 7.1 mm for site Kidr in the October 2002, Table 7-2 (but also now with an exception for the October campaign in 2003, Table 7-5).

As we mentioned above (see Figures 5-3 and 5-4), an enormous solar prominence erupted from the Sun on 28th October 2003, which date coincided with the tenth GPS campaign (from October 28 to November 1). The associated coronal mass ejection came out from the Sun's surface at about 2,300 km per second and it stirs up the strong ionosphere activity /Brekke, 2003/, which affected accuracy of the GPS measurements. Table 7-5 shows that the horizontal and vertical precisions were about 3 and 6 mm, respectively, which was up to two times the normal RMS. It is obvious that the local ionosphere models used together with the L1 observable could not really model such a strong and variable ionospheric activity.

In order to test the local ionosphere modelling, we used also the ionosphere-free linear combination (L3) in the October 2003 campaign. The results are listed in Table 7-7. To our surprise, the internal precision of L3 was several times better than for the L1 observable (see Table 7-5). (One should bear in mind that the L3 observable is usually more than 3 times noisier than the L1 observable.) It seems that the local ionosphere model cannot reflect the short-term TEC variations (see Figures 4-2 and 4-3), especially in the ionosphere maximum period. For this reason, the combination L3 was also applied in all eleven GPS campaigns from 2000 to 2004. Some of these results of the internal precisions from 2002 to 2004 are listed in Tables 7-8 to 7-11. In most cases the horizontal precisions is smaller than those using the L1 observable. However, the vertical precisions were not much improved, and sometimes it still was about 6 mm (see Table 7-10). For the June campaign

of 2003 (see Tables 7-4 and 7-10) the results were slightly better for the L1 compared to L3 observable, and this could possibly be explained by the fact that the ionosphere was calm, yielding a reliable local ionosphere model.

There is (at least) a third way to process the GPS data for a small network, namely the L1 and L2 phase observables can be used simultaneously as input data to the network adjustment. The results of the internal precisions are listed in Table 7-12 for the October campaign 2003. The precisions, using the observable L1 and L2 together, were slightly worse than those using only the L1 observable (in comparison to Table 7-5). This can be explained by that a) the higher noise level for the L2 observable /Hugentobler et al, 2001/ was not considered, and b) the local ionosphere model used was the one for L1, which is not the same for L2.

The precisions of the longest baseline from Knip to Oskarshamn (about 60 km long), determined by the L3 observable, were almost the same as or even better than those of the short baselines of the local network using only observable L1 (see Tables 7-2 to 7-6). It is likely that there were some unmodelled ionosphere bias in the regional model used with L1. The regional ionosphere models are of a very long wavelength nature /Rothacher et al, 1996/ with some limited precision, particularly in a rapidly variable ionosphere. When using observable L3 the precisions were almost the same for both short and long baselines (see the Tables 7-7 to 7-11).

As we mentioned above (see the Section 5.2) two Trimble receivers with some old internal software were used in October 2002. A special test, with exchange of receivers with old and updated internal software was performed. As shown from the Tables 7-2 and 7-7, no systematic error is introduced by changing between these different types of software.

Due to a power/battery failure at site Karr in October 2003 a four-hour data set was lost, but the estimated precision was not affected (see Tables 7-5 and 7-7).

Table 7-2. Daily coordinate residuals vs the total static network adjustment of the October 2002 GPS campaign using the L1 observable. Station Knip is held fixed. The last column is the RMS of the residuals. Unit is mm.

Station		1st session	2nd session	3rd session	4th session	5th session	RMS
Djup	N–S	–0.4	–0.9	1.5	–0.9	0.7	1.0
	E–W	0.0	–0.4	1.0	–1.0	1.6	1.1
	Up	4.0	2.0	3.7	–3.2	–10.4	6.2
Gang	N–S	–0.5	–0.4	0.2	0.1	0.7	0.5
	E–W	0.0	0.2	–0.5	0.6	–0.8	0.6
	Up	–1.2	0.0	0.3	1.2	–1.8	1.2
Gran	N–S	–0.4	–1.1	0.8	–0.3	1.7	1.1
	E–W	–0.3	0.0	0.0	0.5	–0.6	0.4
	Up	0.2	1.5	3.6	–1.2	–10.4	5.6
Karr	N–S	–0.6	–1.3	0.7	–0.2	2.0	1.3
	E–W	–0.2	0.1	–0.2	0.7	–0.8	0.6
	Up	2.6	1.0	3.7	–0.7	–10.7	5.9
Kidr	N–S	–0.7	–0.7	1.5	–1.0	0.7	1.1
	E–W	0.1	–0.7	1.4	–1.5	2.5	1.7
	Up	6.7	1.4	4.5	–3.6	–11.2	7.1
Stor	N–S	0.4	0.2	0.3	–0.7	–0.2	0.4
	E–W	0.3	–0.6	1.3	–1.7	3.2	0.9
	Up	1.5	0.3	0.5	–1.6	–0.4	1.1
Oskarshamn	N–S	–0.5	0.1	–0.1	–0.1	0.9	0.5
	E–W	0.0	0.1	0.5	–0.6	–0.2	0.4
	Up	4.3	–1.6	–0.9	–1.2	2.7	2.8

Table 7-3. Daily station coordinate residuals vs the combined solution for the February campaign in 2003 with L1 observables. Station Knip is held fixed. Unit is mm.

Station		1st session	2nd session	3rd session	4th session	RMS
Djup	N–S	–0.8	–0.4	1.6	–0.1	1.1
	E–W	–0.4	–0.7	1.1	0.8	0.9
	Up	–0.6	0.6	0.0	–1.3	0.9
Gang	N–S	–0.7	–0.2	0.6	0.3	0.6
	E–W	0.2	0.1	0.2	–0.3	0.2
	Up	1.9	–0.5	1.5	–1.4	1.2
Gran	N–S	–1.4	–0.6	1.4	1.3	1.4
	E–W	–0.5	–0.6	1.3	0.4	0.9
	Up	1.4	–1.1	1.5	–1.4	1.6
Karr	N–S	–0.9	–0.4	1.2	0.5	0.9
	E–W	–0.4	–0.6	1.4	0.1	0.9
	Up	1.2	–1.2	0.9	–0.8	1.2
Kidr	N–S	–0.8	–0.3	1.6	–0.4	1.1
	E–W	–0.4	–0.9	1.2	0.9	1.0
	Up	–0.2	0.3	–2.2	1.9	1.7
Stor	N–S	0.1	0.3	–0.4	–0.4	0.3
	E–W	0.4	0.0	–0.3	0.0	0.3
	Up	–0.1	1.1	–3.3	3.2	2.7
Oskarshamn	N–S	0.9	–0.1	0.0	0.1	0.5
	E–W	0.5	0.0	0.0	0.1	0.3
	Up	–3.9	–1.0	–0.5	3.0	2.9

Table 7-4. Daily station coordinate residuals vs the combined solution for the June campaign in 2003 using L1 observable. Station Knip is held fixed. Unit is mm.

Station		1st session	2nd session	3rd session	4th session	5th session	RMS
Djup	N–S	0.3	–1.1	0.8	–1.0	1.3	1.1
	E–W	–0.4	1.6	0.3	–0.9	0.9	1.0
	Up	6.3	2.0	1.0	–2.9	–2.9	3.9
Gang	N–S	–0.3	0.4	0.1	–0.5	0.6	0.5
	E–W	–0.4	–0.3	0.5	0.0	–0.3	0.4
	Up	–0.7	0.6	1.5	–0.5	–1.3	1.1
Gran	N–S	–0.8	–0.5	0.8			0.9
	E–W	–0.5	0.7	–0.1			0.6
	Up	0.8	1.1	1.8			1.6
Karr	N–S	–1.2	–0.9	0.3	0.3	1.1	0.9
	E–W	–0.4	0.2	0.0	0.3	–0.5	0.3
	Up	2.1	0.7	1.0	–1.8	–0.2	1.5
Kidr	N–S	0.1	–0.7	0.3			0.6
	E–W	–0.9	1.7	0.1			1.3
	Up	3.2	0.4	–1.4			2.5
Stor	N–S	1.0	–0.6	–0.4			0.8
	E–W	0.5	0.6	0.2			0.6
	Up	4.3	–0.8	–1.4			3.2
Oskarshamn	N–S	0.0	–0.7	0.8	0.3	–1.5	0.9
	E–W	0.3	0.3	0.1	–0.6	0.0	0.4
	Up	2.6	–3.9	0.9	4.7	–10.8	6.3
Äspö	N–S			0.4	–0.3	0.5	0.5
	E–W			1.2	–0.1	–1.2	1.2
	Up			–0.5	–2.6	2.4	2.5
Bast	N–S			–1.1	–0.5	2.0	1.7
	E–W			–3.9	–0.2	1.7	3.0
	Up			1.9	–1.9	–1.0	2.0
OKG	N–S			–1.3	0.5	0.1	1.0
	E–W			1.8	–0.4	–1.3	1.6
	Up			–0.7	–3.8	4.7	4.3

Table 7-5. Daily station coordinate residuals vs the combined solution for the October campaign in 2003 using L1. Station Knip is fixed. Unit is mm.

Station		1st session	2nd session	3rd session	4th session	5th session	RMS
Djup	N–S	–2.4	–3.3	–0.8	3.2	4.5	3.4
	E–W	0.6	3.5	–2.2	–1.5	–0.7	2.2
	Up	7.1	–8.6	–1.6	6.1	–0.2	6.4
Gang	N–S	–0.2	0.7	–0.7	0.3	–0.6	0.6
	E–W	0.3	–0.8	0.9	0.2	–0.9	0.8
	Up	1.6	–2.8	–1.1	1.0	4.2	2.8
Gran	N–S	–1.6	–0.7	–0.8			1.4
	E–W	0.6	0.4	–0.1			0.5
	Up	7.9	–7.2	–0.9			7.6
Karr	N–S	–1.8	0.0	–1.4	1.6	1.3	1.5
	E–W	0.8	0.1	0.6	–0.2	–2.0	1.1
	Up	3.7	–8.6	0.0	3.9	5.8	5.8
Kidr	N–S	–0.4	–2.2	0.5			1.6
	E–W	–0.4	3.7	–3.1			3.4
	Up	11.0	–8.2	–3.0			9.9
Stor	N–S	1.0	–1.8	0.7			1.5
	E–W	0.3	–3.4	2.2			2.9
	Up	0.3	–3.7	1.0			2.7
Oskarshamn	N–S	–1.0	–0.4	0.0	1.3	–0.6	0.9
	E–W	0.8	0.5	–0.2	–0.3	–0.8	0.6
	Up	7.0	–5.2	–1.2	4.5	–4.3	5.4
Äspö	N–S			0.6	1.4	–0.6	1.2
	E–W			3.0	0.2	–2.6	2.8
	Up			–0.4	1.9	4.5	3.5
Bast	N–S			1.7	–0.1	0.5	1.3
	E–W			–1.2	–1.1	0.9	1.3
	Up			–0.3	2.7	3.9	3.3
OKG	N–S			3.2	0.8	–1.8	2.7
	E–W			4.7	–0.1	–2.6	3.8
	Up			–0.8	1.3	7.2	

Table 7-6. Daily station coordinate residuals vs the combined solution for the March campaign in 2004 using L1 observables. Station Knip is held fixed. Unit is mm.

Station		1st session	2nd session	3rd session	4th session	5th session	RMS
Djup	N–S			2.8	–1.3	–1.0	2.3
	E–W			–2.5	0.8	1.9	2.3
	Up			3.0	–2.2	2.5	3.2
Gang	N–S	0.7	–0.2	–0.2	–0.1	0.4	0.4
	E–W	–0.1	–0.2	0.6	–0.4	0.3	0.4
	Up	–2.0	0.5	0.4	0.6	–0.1	1.1
Gran	N–S	0.0	–0.3	1.2			0.9
	E–W	0.7	–0.4	0.0			0.6
	Up	–3.9	0.8	3.2			3.6
Karr	N–S	0.5	–0.3	0.3			0.4
	E–W	0.4	–0.2	0.1			0.3
	Up	–3.5	1.2	1.3			2.8
Kidr	N–S	–1.2	–0.3	3.4			2.6
	E–W	1.4	–0.5	–0.9			1.2
	Up	–3.2	1.3	3.1			3.3
Stor	N–S	–1.2	–0.1	2.1			1.7
	E–W	0.9	–0.2	–1.2			1.1
	Up	0.4	0.2	–0.6			0.5
Oskarshamn	N–S	0.0	0.1	–0.2	–0.6	1.9	1.0
	E–W	0.0	0.2	0.1	–0.7	1.3	0.8
	Up	0.5	1.9	–1.8	–1.1	1.9	1.7
Äspö	N–S			–1.3	0.2	1.6	1.5
	E–W			1.3	–0.9	0.6	1.2
	Up			–0.4	1.9	4.5	3.5
Bast	N–S			–0.6	0.0	0.7	0.6
	E–W			–0.8	0.4	0.3	0.7
	Up			0.4	–0.1	0.4	0.4
OKG	N–S			–3.1	0.9	2.2	2.7
	E–W			2.5	–1.2	–0.3	2.0
	Up			–3.7	1.4	2.1	3.2

Table 7-7. Daily station coordinate residuals vs the combined solution for the October campaign in 2003 using L3 observables. Station Knip is held fixed. Unit is mm.

Station		1st session	2nd session	3rd session	4th session	5th session	RMS
Djup	N–S	0.1	0.1	0.5	–0.3	–0.6	0.5
	E–W	0.0	–0.4	–0.4	0.7	0.1	0.5
	Up	0.8	1.7	–0.8	–0.3	–2.6	1.7
Gang	N–S	–0.2	–0.1	–0.2	0.6	–0.4	0.4
	E–W	–0.5	0.1	0.1	0.0	0.1	0.3
	Up	–2.3	0.2	0.4	–0.7	2.5	1.8
Gran	N–S	0.1	0.1	0.0			0.1
	E–W	–0.2	0.0	–0.1			0.2
	Up	0.2	–0.6	1.7			1.2
Karr	N–S	–0.7	0.4	0.0	0.3	–0.8	0.6
	E–W	–0.5	0.1	0.2	0.2	0.1	0.3
	Up	–2.5	–0.1	2.4	–1.0	–0.4	1.8
Kidr	N–S	0.1	0.0	0.2			0.2
	E–W	0.4	–0.3	–0.7			0.6
	Up	2.1	0.3	–2.3			2.2
Stor	N–S	–0.2	0.0	0.5			0.4
	E–W	0.4	–0.4	–0.7			0.7
	Up	–0.4	0.4	1.1			0.9
Oskarshamn	N–S	–1.0	–0.4	0.0	1.3	–0.6	0.9
	E–W	0.8	0.5	–0.2	–0.3	–0.8	0.6
	Up	7.0	–5.2	–1.2	4.5	–4.3	5.4
Äspö	N–S			0.8	0.2	–1.0	0.9
	E–W			0.7	–0.2	0.0	0.5
	Up			4.9	–1.2	–1.6	3.7
Bast	N–S			0.3	0.2	–0.6	0.5
	E–W			0.1	0.0	0.5	0.4
	Up			–0.2	–0.7	0.7	0.7
OKG	N–S			0.0	0.4	–0.8	0.6
	E–W			0.4	–0.4	0.4	0.5
	Up			–10.7	1.8	3.4	8.1

Table 7-8. Daily site coordinate residuals vs the combined solution for the October campaign in 2002 using L3 observable. Site Knip is held fixed. Unit is mm.

Station		1st session	2nd session	3rd session	4th session	5th session	RMS
Djup	N–S	–0.4	–0.2	0.2	0.3	–0.4	0.3
	E–W	0.4	0.1	–0.2	–0.1	0.1	0.2
	Up	4.8	0.3	–0.6	–0.1	–4.2	3.2
Gang	N–S	–0.2	0.2	–0.3	0.1	0.2	0.2
	E–W	0.1	–0.1	0.1	0.1	–0.4	0.2
	Up	0.0	–0.3	–0.3	0.5	0.0	0.3
Gran	N–S	0.0	0.2	–0.3	0.2	–0.2	0.2
	E–W	–0.1	–0.2	0.2	0.2	–0.4	0.3
	Up	3.1	0.1	–0.6	0.3	–3.4	2.3
Karr	N–S	–0.7	0.1	–0.2	0.3	0.4	0.4
	E–W	0.1	–0.1	0.2	0.1	–0.7	0.4
	Up	12.7	0.9	–0.7	0.5	–8.0	7.5
Kidr	N–S	–0.4	0.0	0.2	0.2	–0.8	0.5
	E–W	0.4	0.1	–0.1	–0.1	0.3	0.2
	Up	7.0	–0.2	–0.3	0.2	–4.4	4.1
Stor	N–S	–0.5	0.1	–0.1	0.0	0.4	0.3
	E–W	0.3	0.0	–0.1	–0.1	0.5	0.3
	Up	1.9	0.3	1.0	–0.7	–4.3	2.4
Oskarshamn	N–S	–0.5	0.1	–0.1	–0.1	0.9	0.5
	E–W	0.0	0.1	0.5	–0.6	–0.2	0.4
	Up	4.3	–1.6	–0.9	–1.2	2.7	2.8

Table 7-9. Daily site coordinate residuals vs the combined solution for the February campaign in 2003 using the L3 observable. Site Knip is held fixed. Unit is mm.

Station		1st session	2nd session	3rd session	4th session	RMS
Djup	N–S	0.0	0.0	0.1	–0.1	0.1
	E–W	0.3	–0.1	0.1	–0.3	0.3
	Up	–1.1	–0.7	0.7	1.7	1.3
Gang	N–S	0.7	0.3	–1.3	0.2	0.9
	E–W	0.3	0.1	–0.2	–0.6	0.4
	Up	1.2	–2.6	4.2	–1.4	3.0
Gran	N–S	0.1	–0.1	–0.2	0.3	0.2
	E–W	–0.1	0.0	0.1	0.0	0.1
	Up	–1.8	0.2	–2.2	4.0	2.8
Karr	N–S	0.5	0.0	0.2	–0.8	0.5
	E–W	0.3	–0.1	0.1	–0.2	0.2
	Up	–2.2	–0.7	–1.0	4.8	3.1
Kidr	N–S	0.1	0.1	–0.3	0.0	0.2
	E–W	0.2	–0.2	0.4	–0.4	0.4
	Up	0.1	–0.2	–1.8	2.2	1.6
Stor	N–S	0.1	0.2	–0.6	0.3	0.4
	E–W	0.3	–0.1	0.0	–0.3	0.3
	Up	–1.4	–2.2	5.6	–2.3	3.8
Oskarshamn	N–S	0.9	–0.1	0.0	0.1	0.5
	E–W	0.5	0.0	0.0	0.1	0.3
	Up	–3.9	–1.0	–0.5	3.0	2.9

Table 7-10. Daily site coordinate residuals vs the combined solution for the June campaign in 2003 using L3 observable. Site Knip is held fixed. Unit is mm.

Station		1st session	2nd session	3rd session	4th session	5th session	RMS
Djup	N–S	0.4	0.4	0.3	–0.6	–0.5	0.5
	E–W	–1.3	–0.1	–0.1	1.0	–0.1	0.8
	Up	3.4	0.6	–1.4	1.5	–3.9	2.8
Gang	N–S	–0.1	0.4	0.1	–0.1	–0.3	0.3
	E–W	0.3	0.9	0.3	–0.3	–0.6	0.6
	Up	–1.8	0.2	1.5	1.7	–4.3	2.6
Gran	N–S	–0.8	0.3	0.8			0.8
	E–W	0.1	0.3	–0.4			0.4
	Up	–3.2	2.1	2.9			3.4
Karr	N–S	–0.7	–0.1	0.3	0.3	0.4	0.5
	E–W	–0.8	0.6	0.7	0.0	0.0	0.6
	Up	–0.3	2.8	0.5	–0.3	–2.0	1.8
Kidr	N–S	0.2	0.5	0.1			0.4
	E–W	–0.9	1.0	–0.5			1.0
	Up	–0.6	0.9	1.1			1.1
Stor	N–S	0.1	0.0	–0.2			0.1
	E–W	–1.6	–0.2	0.8			1.3
	Up	7.2	–4.0	–1.6			5.9
Oskarshamn	N–S	0.0	–0.7	0.8	0.3	–1.5	0.9
	E–W	0.3	0.3	0.1	–0.6	0.0	0.4
	Up	2.6	–3.9	0.9	4.7	–10.8	6.3
Äspö	N–S			0.1	–0.1	0.2	0.2
	E–W			0.5	–0.4	–0.1	0.5
	Up			–1.4	–0.6	0.9	1.2
Bast	N–S			–4.3	–0.3	3.5	3.9
	E–W			–5.6	0.7	1.6	4.1
	Up			–0.6	–1.0	1.1	1.1
OKG	N–S			–0.8	0.4	0.3	0.7
	E–W			0.7	–0.6	0.0	0.6
	Up			–0.4	–0.8	0.2	0.7

Table 7-11. Daily site coordinate residuals vs the combined solution for the March campaign in 2004 using L3 observables with site Knip held fixed. Unit is mm.

Station		1st session	2nd session	3rd session	4th session	5th session	RMS
Djup	N–S			–0.6	0.2	0.8	0.7
	E–W			–0.7	0.0	1.6	1.2
	Up			0.3	0.0	0.1	0.2
Gang	N–S	0.2	–0.1	–0.4	0.3	0.7	0.4
	E–W	–0.4	–0.2	0.0	0.0	1.1	0.6
	Up	1.4	0.8	–1.0	–0.4	0.3	1.0
Gran	N–S	–0.5	0.1	0.3			0.4
	E–W	0.1	–0.3	0.1			0.2
	Up	0.8	–0.2	1.0			0.9
Karr	N–S	0.6	–0.2	–0.8			0.7
	E–W	0.0	–0.2	–0.1			0.2
	Up	0.3	0.0	0.4			0.4
Kidr	N–S	–0.7	0.0	1.2			1.0
	E–W	–0.7	0.2	0.5			0.6
	Up	–0.4	–0.1	3.6			2.6
Stor	N–S	–0.7	0.0	0.9			0.8
	E–W	–0.5	0.1	0.3			0.4
	Up	–0.3	–0.7	4.2			3.0
Oskarshamn	N–S	0.0	0.1	–0.2	–0.6	1.9	1.0
	E–W	0.0	0.2	0.1	–0.7	1.3	0.8
	Up	0.5	1.9	–1.8	–1.1	1.9	1.7
Äspö	N–S			–0.9	0.0	1.9	1.5
	E–W			0.1	–0.3	1.4	1.0
	Up			–0.8	0.1	1.4	1.1
Bast	N–S			–0.8	0.0	1.3	1.1
	E–W			0.2	0.1	0.1	0.2
	Up			2.1	0.7	–5.9	4.4
OKG	N–S			–0.6	–0.1	1.5	1.1
	E–W			0.3	–0.2	0.8	0.7
	Up			–0.9	–0.2	1.7	1.4

Table 7-12. Daily site coordinate residuals vs combined solution for the October campaign in 2003 using L1 and L2 observables. Unit is mm.

Station		1st session	2nd session	3rd session	4th session	5th session	RMS
Djup	N–S	–3.3	–4.4	–1.2	4.3	6.0	4.6
	E–W	0.9	4.7	–3.1	–2.0	–0.7	3.0
	Up	4.9	–17.2	10.5	6.7	–3.3	11.0
Gang	N–S	–0.4	1.1	–0.7	0.1	–0.7	0.8
	E–W	0.6	–0.9	0.4	0.6	–1.1	0.9
	Up	–1.5	–5.3	7.7	–1.4	2.8	5.0
Gran	N–S	–2.4	–0.5	–1.6			2.1
	E–W	0.9	0.4	–0.3			0.7
	Up	2.3	–12.0	12.8			12.5
Karr	N–S	–2.3	0.3	–1.9	2.0	1.8	2.0
	E–W	1.4	0.0	–0.1	0.2	–2.4	1.4
	Up	–2.5	–15.2	17.8	–1.0	4.5	12.0
Kidr	N–S	–0.6	–3.3	1.8			2.7
	E–W	–0.6	4.9	–3.9			4.4
	Up	12.5	–10.9	–4.1			12.1
Stor	N–S	1.3	–2.3	1.2			2.1
	E–W	–1.0	4.5	–1.4			3.4
	Up	–2.0	–3.0	–12.8			9.4
Oskarshamn	N–S	–1.0	–0.4	0.0	1.3	–0.6	0.9
	E–W	0.8	0.5	–0.2	–0.3	–0.8	0.6
	Up	7.0	–5.2	–1.2	4.5	–4.3	5.4
Äspö	N–S			3.1	1.2	–1.2	2.5
	E–W			1.4	1.1	–2.9	2.4
	Up			37.0	–6.8	–3.0	26.7
Bast	N–S			2.9	–0.5	0.7	2.1
	E–W			–1.7	–1.5	1.6	2.0
	Up			11.0	1.6	–0.6	7.9
OKG	N–S			4.5	0.7	–2.0	3.5
	E–W			4.6	0.5	–3.2	3.9
	Up			24.0	–4.1	2.3	17.3

7.2 Preliminary analysis of the combined GPS solutions

In the above section the internal precisions were analysed. However, such an analysis tells you little about the absolute accuracy of point determination, but essentially gives you the scatter among the observations within each observation campaign. We will now assume that there are no internal motions among the stations of our network, but the total network may move as a solid block from one epoch campaign to another. The velocity model of the ITRF97 will be used to propagate all epoch solutions to the common epoch 2002.0. By comparing the solutions for coordinates of these individual solutions, we get a rough idea about the basic accuracy of these solutions under the assumption of no internal motions within the network.

The differences from a combined solution of all eleven individual campaign solutions from 2000 to 2004 are listed in Tables 7-13 and 7-14, processed by the observables L1 and L3, respectively. In general, the RMS values of horizontal coordinates are of the order of 1–2 mm. From the tables we can see that the horizontal coordinate residuals (the coordinate differences from the mean values) of four stations (Djup, Karr, Kidr and Stor) are as large as about 4 mm in the last two campaigns. These residuals may indicate that there are some real tectonic deformations, but they could also be the result of non-detected/eliminated temporal systematic effects. (cf Section 5.2) As one could expect, the vertical errors of about 4 mm

are somewhat larger than those in the horizontal components. In particular, the large vertical RMS of 13.7 mm at site Djup is remarkable. Again, this might be an indication of real vertical motions. Hence, we conclude that there are significant un-modelled biases in the static adjustment models. In Chapters 8 and 9 the data will be adjusted with the inclusion of linear temporal changes of the coordinates in the adjustment model.

Table 7-13. The coordinate differences from the mean values of the eleven epoch GPS campaigns using the observable L1, transformed to the common epoch (2002.0). Unit is mm.

Site	Epoch	1	2	3	4	5	6	7	8	9	10	11	RMS
Djup	North	–0.3	–0.1	–1.1	–2.0	0.9	1.4	–0.7	1.5	–0.6	–0.3	4.2	1.7
	East	–0.0	–0.8	–0.2	0.2	–0.9	0.7	0.9	1.7	–0.6	1.0	–1.9	1.0
	Up	–22.1	–21.0	–20.1	7.4	4.7	7.0	9.7	10.5	7.8	5.5	10.7	13.7
Gang	North	1.0	0.6	–0.6	0.2	–0.6	0.5	–0.3	–0.9	–0.4	0.1	0.7	0.6
	East	0.3	0.3	–0.9	0.1	0.3	0.2	0.1	–0.9	0.0	1.0	–0.4	0.5
	Up	1.1	–5.7	–0.2	–0.9	–0.1	0.2	1.7	3.5	–1.5	–0.5	2.6	2.4
Karr	North	–0.5	0.1	–0.8	–1.5	–1.3	–0.7	0.1	–1.9	–0.7	4.1	3.1	1.9
	East	1.4	0.5	–0.3	0.7	–0.1	–0.6	–0.1	1.1	–1.0	0.1	–1.7	0.9
	Up	0.5	0.5	–0.4	4.6	0.1	0.6	4.5	3.8	–2.1	–6.7	–5.3	3.6
Kidr	North	3.6	1.4	1.5	–0.9	2.1	2.1	1.0	–1.8	0.1	–4.4	–4.7	2.7
	East	0.2	0.2	0.7	0.0	–2.0	–1.2	0.3	1.1	–0.6	0.4	0.8	0.9
	Up	–2.6	–2.6	–1.4	2.3	–1.2	4.1	1.8	0.9	2.1	–2.1	–1.3	2.3
Gran	North	0.9	0.8	–0.6	0.9	0.3	0.4	0.5	–1.6	–0.6	0.2	–1.1	0.8
	East	0.2	0.7	0.5	–0.4	–0.3	–0.9	0.6	0.3	–1.2	–0.7	1.5	0.8
	Up	0.8	1.7	1.8	4.5	–0.6	–2.5	1.4	3.0	–0.7	–5.0	–3.9	2.9
Stor	North	1.6	0.7	1.8	–0.5	–0.3	3.1	0.4	0.4	0.5	–4.2	–3.3	2.1
	East	0.9	–0.1	1.3	–0.8	–0.5	1.5	2.0	0.3	–0.9	–1.3	–2.4	1.3
	Up	–0.1	4.2	8.2	–0.4	–0.3	–2.4	–2.5	–1.8	3.3	–2.0	–6.4	4.0
Äspö	North									2.5	–2.3	–0.1	2.4
	East									1.1	0.5	–1.6	1.4
	Up									–0.9	–0.5	1.4	1.2
Bast	North									–1.3	0.5	0.8	1.1
	East									–1.1	1.9	–0.8	1.7
	Up									8.5	–3.8	–4.7	7.4
OKG	North									2.4	–2.2	–0.2	2.3
	East									–0.9	1.9	–1.0	1.7
	Up									0.1	–2.8	2.8	2.8

Table 7-14. The coordinate differences from the mean values of the eleven epoch campaigns using the L3 observable, transformed to the common epoch (2002.0): Unit is mm.

Site	Epoch	1	2	3	4	5	6	7	8	9	10	11	RMS
Djup	North	–0.2	0.2	–0.7	–1.1	3.9	1.9	–1.2	–0.9	–0.7	–0.5	–0.8	1.5
	East	–0.1	–1.0	–0.7	–0.7	–1.1	1.3	0.3	–0.7	1.2	2.3	–0.9	1.1
	Up	–27.4	–26.7	–25.2	8.4	6.4	7.6	12.6	14.8	13.2	9.1	7.2	17.2
Gang	North	1.9	0.1	–0.9	3.2	–1.5	1.8	–0.1	–3.6	0.1	–0.9	0.0	1.8
	East	0.0	–0.9	–1.3	–0.4	0.3	1.1	1.6	–1.1	1.5	2.0	–2.8	1.5
	Up	0.3	–5.0	–3.6	–0.9	–1.2	0.9	–1.2	0.9	0.3	8.6	–2.5	3.6
Karr	North	–1.8	–0.6	–2.2	–2.1	–2.7	–1.3	2.8	–5.9	–1.9	8.6	7.0	4.4
	East	3.2	–0.8	–0.7	1.5	1.3	1.7	–0.1	1.8	–0.6	0.0	–7.4	2.8
	Up	0.5	0.0	–2.6	5.0	3.2	1.7	0.8	3.3	–0.7	–5.6	–5.6	3.4
Kidr	North	4.6	2.6	2.9	0.1	3.7	3.1	1.9	–3.1	0.1	–8.2	–7.6	4.4
	East	1.1	1.9	1.6	0.7	–1.3	–1.6	–0.3	–2.9	–0.9	1.5	0.1	1.5
	Up	–5.1	–2.0	–3.8	2.1	–0.8	1.6	1.0	0.7	0.7	2.5	3.1	2.7
Gran	North	0.7	1.7	0.2	1.8	–0.1	0.6	1.1	–3.1	0.0	–0.6	–2.3	1.5
	East	1.3	2.1	2.8	–3.8	1.2	–1.9	2.8	–2.2	–0.5	–2.8	0.9	2.4
	Up	0.6	4.4	2.3	0.1	0.6	–3.1	–2.7	3.0	–1.1	–3.2	–0.8	2.5
Stor	North	1.6	0.7	1.8	–0.5	–0.3	3.1	0.4	0.4	0.5	–4.2	–3.3	2.1
	East	0.9	–0.1	1.3	–0.8	–0.5	1.5	2.0	0.3	–0.9	–1.3	–2.4	1.3
	Up	–0.1	4.2	8.2	–0.4	–0.3	–2.4	–2.5	–1.8	3.3	–2.0	–6.4	4.0
Äspö	North									2.5	–2.3	–0.1	2.4
	East									1.1	0.5	–1.6	1.4
	Up									–0.9	–0.5	1.4	1.2
Bast	North									–1.3	0.5	0.8	1.1
	East									–1.1	1.9	–0.8	1.7
	Up									8.5	–3.8	–4.7	7.4
OKG	North									2.4	–2.2	–0.2	2.3
	East									–0.9	1.9	–1.0	1.7
	Up									0.1	–2.8	2.8	2.8

8 Baseline length evolutions

This chapter is devoted to the analysis of the temporal changes of baseline lengths of the network. As in /Sjöberg et al, 2002/ we start to present a simple theory for estimating the linear change of a baseline (or coordinate) with time from epoch-wise data. Then we apply the theory to estimate the expected accuracy of the estimated parameters with time, and finally, we use the theory to the real data from the Äspö network.

8.1 Theory: Linear regression of station/baseline velocities

Let the observation equations

$$y_i - \varepsilon_i = a + bt_i \; ; \; i = 1, \cdots, n \tag{5}$$

represent the temporal evolution of a coordinate or baseline length. Here y_i is the observation with the random observation error ε_i, observed at epoch t_i and totally n times. The constants a and b are the unknown parameters of the equation, where a is the coordinate/baseline at time $t_i = 0$, while b is the coordinate change with time. All the observation equations can be expressed by the matrix equation

$$AX = L - \varepsilon, \tag{6a}$$

where

$$A^T = \begin{pmatrix} 1 & 1 & \dots & 1 \\ t_1 & t_2 & \dots & t_n \end{pmatrix}, \qquad X = \begin{pmatrix} a \\ b \end{pmatrix}, \tag{6b}$$

$$L^T = (y_1 \;\; y_2 \cdots \;\; y_n) \tag{6c}$$

and

$$\varepsilon^T = (\varepsilon_1 \; \varepsilon_2 \cdots \;\; \varepsilon_n). \tag{6d}$$

Here superscript T denotes the transpose of the matrix. If we assume that all observation errors are random and uncorrelated with expectation zero, the least squares solution of the system (6) becomes /Bjerhammar, 1973; Sjöberg, 1984; see also Sjöberg, 1982, pp 19–22/:

$$\hat{X} = \begin{pmatrix} \hat{a} \\ \hat{b} \end{pmatrix} = (A^T A)^{-1} A^T L = \begin{pmatrix} n & \sum_{i=1}^{n} t_i \\ \sum_{i=1}^{n} t_i & \sum_{i=1}^{n} t_i^2 \end{pmatrix}^{-1} \begin{pmatrix} \sum_{i=1}^{n} y_i \\ \sum_{i=1}^{n} t_i y_i \end{pmatrix}, \tag{7a}$$

with the covariance matrix

$$Q_{\hat{X}\hat{X}} = \sigma_0^2 (A^T A)^{-1} = \sigma_0^2 \begin{pmatrix} n & \sum_{i=1}^{n} t_i \\ \sum_{i=1}^{n} t_i & \sum_{i=1}^{n} t_i^2 \end{pmatrix}^{-1}, \tag{7b}$$

where σ_0^2 is the so-called variance of unit weight, which can be estimated by the formula

$$\hat{\sigma}_0^2 = \frac{\sum_{i=1}^{n} (y_i - \hat{a} - \hat{b} t_i)^2}{n-2} \tag{8}$$

If t_i is substituted by $\Delta t_i = t_i - t_0$, where t_0 is the mean epoch of the total time interval, it implies that $\sum_{i=1}^{m} \Delta t_i = 0$, and Equations (7a) and (7b) can be simplified to

$$\hat{X} = \begin{pmatrix} \hat{a} \\ \hat{b} \end{pmatrix} = \begin{pmatrix} \frac{1}{n} \sum_{i=1}^{n} y_i \\ \frac{\sum_{i=1}^{n} \Delta t_i y_i}{\sum_{i=1}^{n} (\Delta t_i)^2} \end{pmatrix} \tag{9}$$

and

$$Q_{\hat{X}\hat{X}} = \hat{\sigma}_0^2 \begin{pmatrix} n^{-1} & 0 \\ 0 & \left(\sum_{i=1}^{n} (\Delta t_i)^2 \right)^{-1} \end{pmatrix} \tag{10}$$

Of particular interest to our study are the standard errors of the estimated coordinate (a) and its temporal change (b) obtained from Equation (10):

$$\hat{\sigma}_{\hat{a}} = \frac{\hat{\sigma}_0}{\sqrt{n}} \tag{11a}$$

and

$$\hat{\sigma}_{\hat{b}} = \frac{\hat{\sigma}_0}{\sqrt{\sum_{i=1}^{n} (\Delta t_i)^2}}; \tag{11b}$$

As one would expect, these formulas show that

- The precisions increase with the number of observations and the total time span.
- $\hat{\sigma}_a$ and $\hat{\sigma}_b$ are proportional to the standard errors $\hat{\sigma}_0$ of the GPS measurements.

To judge whether the estimated velocity $\hat{b}$ is significant or not, a Student's t-test can be used /see e.g. Koch, 1999/. The t-statistic, based on the estimator $\hat{b}$ and its error estimate $\hat{\sigma}_b$:

$$t = \frac{\hat{b}}{\hat{\sigma}_b}, \tag{12}$$

is to be compared to its theoretical value $t_{\alpha/2}$ (n–2) given by the two-sided t-distribution, where n is the number of observation epochs and α is the chosen risk level. Our null-hypothesis is that there is no motion, i.e. H_0: b = 0. If $|t| \leq t_{\alpha/2}$, then H_0 is accepted, otherwise rejected.

8.2 Expected precision of the Äspö network on a long-time basis

The results of the previous section can be applied to derive expected precision values of the coordinates and site velocities of the network. The Equations (11 a, b) give us all of the relations of interest. In the real case we have seen that the Äspö network estimation has a precision (σ_0) of a single coordinate estimation of 1–1.5 mm and ca 4 mm in the horizontal and vertical components, respectively (see Tables 7-2 to 7-11), and the frequency of measurements were three times per year. Inserting these figures into Equations (11a, b) we obtain the results of Table 8-1 for the observation periods of 2 to 5 years. If one requires that the standard error of $\hat{\sigma}_b$ should be within 0.3 mm/yr, this goal is reached after three years of observations, if the standard error of the GPS observations (σ_0) is 1.5 mm. In the same way, assuming that the epoch-wise observed vertical coordinate is precise to 4 mm, it takes more than 5 years until the standard error of its estimated change rate is within 0.3 mm/yr. As there by now are 11 epoch campaigns of less than a 4-year span, it should be possible to get some figures of the local horizontal movements, while the precision of any vertical rate of motion may still be too low.

Comparing the time evolutions of the standard errors for coordinate estimation and velocity estimation ($\hat{\sigma}_a$ and $\hat{\sigma}_b$) of Table 8-1, one can see that the latter decreases more rapidly with time than the former. As we are particularly interested in the precision of the estimated baseline or coordinate change with time, this is a good experience.

All the above results were obtained under the assumption of no correlations among the data. If the data are correlated we should expect that the standard errors of estimated parameters (a and b) will increase.

Table 8-1. Expected precisions of the velocities and coordinates/baselines after 2 to 5 years of observation period with different data qualities σ_0. n = number of epochs.

		σ_b (mm/yr)			σ_a (mm)		
		σ_0 (mm)			σ_0 (mm)		
Yr	N	1	1.5	4	1	1.5	4
2	7	0.31	0.47	1.26	0.41	0.61	1.63
3	10	0.18	0.27	0.71	0.33	0.50	1.33
4	13	0.12	0.18	0.47	0.29	0.43	1.15
5	16	0.09	0.13	0.34	0.26	0.39	1.03

8.3 Estimated change rates of baseline lengths

As the network has been observed for almost four years and there are eleven repeated measurements, the temporal deformation changes of each baseline can be estimated from the baseline estimates of each epoch campaign by simple linear regression (Equations 9 and 10). There are 21 dependent baseline lengths in total (with exclusion of the new sites Äspö, Bast and OKG). The estimated movement rates of the baseline lengths and their precisions are summarized in Table 8-2 using observables L1 and L3. The table shows also the estimated Student's t-statistics to be used in judging whether the estimated velocities are significant or not. These t-values should be compared with its theoretical value $t_{2.5\%}(9) = 2.26$. Hence, if $|t| \leq 2.26$, the hypothesis H_0 (no motion) is accepted, otherwise H_0 is rejected. The table shows that for seven baselines analysed by L1 and two baselines by L3 H_0 is rejected, i.e. their estimated rates of change are statistically significant at the confidence level of 95%. In general, the precisions estimated by the observable L3 are slightly worse than those by L1. This can be explained by the fact that L3 increases the observation noise 3.6 times compared to L1. An additional explanation could be that L3 is more prone to antenna bias than L1, caused by possible change of antenna between campaigns. As a result, only the rate of one of the small baselines is significant for L3. For the long baseline Knip–Oskarshamn, where probably ionosphere bias is a dominant error source in L1, only the L3 signal is useful. All eight significant baseline rates are presented in Figures 8-1 to 8-8. The figures also show that the standard errors of unit weight of each baseline estimate vary between 0.7 and 2.0 mm. Hence, on the average we may say that the epoch-wise estimated baseline length is good to ca 1–1.5 mm.

The baseline change rates were also estimated by the program ADDNEQ of the Bernese software. This implies that all the data are jointly adjusted, which should lead to somewhat better results than the above regression analysis from baseline by baseline. The results are listed in Table 8-3. In the table the standard errors have been scaled up by a factor 10 due to the fact the software neglects the existing correlations among the huge number of GPS data /Sjöberg et al, 2002/. Unfortunately, the scale factor is somewhat tentative, and not directly provided by the adjustment. Comparing with Table 8-2 it can be seen that this factor yields slightly worse error estimates than those by regression analysis. Furthermore, the theoretical t-value to be used in the t-test is not obvious from the network adjustment. For simplicity we will use the same theoretical t-value (2.26) as provided in the regression analysis above. Then, in addition to the long baseline Knip–Oskarshamn only three baselines Knip–Kidr, Gran–Karr and Karr–Kidr change significantly. If the scale factor is reduced to 7 only one more baseline rate (Gang–Karr) becomes significant. Hence, the somewhat uncertain scale factor is not a main cause to explain the different outcomes of Tables 8-2 and 8-3. Hence, the joint adjustment of all the data (Table 8-3) provides a slight alternative solution compared to the epoch-wise adjusted baseline estimates of Table 8-2; the latter yielding up to four significant rates of baseline change within the local net. The long baseline from Knip to Oskarshamn changes significantly in both tests. Interestingly, Table 8-3 shows that while the average standard errors of the baseline rate estimates are of the order of 0.6 mm/yr, the standard errors of the baselines related with significant changes are 2–3 times smaller. The combination of relatively large rates of change and small standard errors give confidence to the results for the outstanding baselines.

Figure 8-9 is based on the results of Table 8-3. It shows some possible slips and rotations of blocks. However, we consider the results too poor to be further studied at this point (cf Chapter 9).

So far the tests were performed with a risk level of 5%. If we decrease the risk level to 1%, the t-value becomes 3.25, implying that only the baseline from Karr to Kidr changes significantly in the regression analysis, while the previous three baselines still change significantly in the Bernese software analysis. (Now, the rate of change of the long baseline (from Oskarshamn to Knip) is significant only in the Bernese software analysis).

Table 8-2. Change rates of 21 dependent baseline lengths for the Äspö network. The estimated rates and their precisions are obtained by linear regression of all eleven campaigns from 2000 to 2004. The estimated rates in bold figures are statistically significant at the confidence level of 95% ($t_{2.5\%}(9) = 2.26$).

Baseline	Observable L1 Rate (mm/yr)	Accuracy (mm/yr)	Length (km)	$\lvert t \rvert = \frac{\hat{b}}{\hat{\sigma}_b}$	Observable L3 Rate (mm/yr)	Accuracy (mm/yr)	Length (km)	$\lvert t \rvert = \frac{\hat{b}}{\hat{\sigma}_b}$
Knip–Djup	0.32	±0.43	3.5	0.74	–0.48	±0.32	3.5	1.50
Knip–Kidr	–1.10	±0.36	4.7	3.05	–1.10	±0.60	4.7	1.83
Knip–Gran	–0.38	±0.16	2.2	2.37	–0.48	±0.32	2.2	1.50
Knip–Karr	0.44	±0.33	2.1	1.33	0.92	±0.70	2.1	1.31
Knip–Gang	–0.06	±0.20	1.5	0.3	–0.07	±0.40	1.5	0.17
Knip–Stor	0.45	±0.27	4.1	1.66	1.0	±0.58	4.1	1.72
Djup–Gang	0.23	±0.36	4.4	0.63	–0.10	±0.37	4.4	0.27
Djup–Gran	–0.01	±0.04	3.2	0.25	–0.09	±0.07	3.2	1.28
Djup–Karr	–0.46	±0.19	3.8	2.42	–0.80	±0.60	3.8	1.33
Djup–Kidr	–0.74	±0.38	1.3	1.94	0.16	±0.20	1.3	0.80
Djup–Stor	1.63	±0.52	2.4	3.13	1.34	±0.87	2.4	1.54
Gang–Granr	–0.21	±0.24	1.7	0.87	–0.11	±0.39	1.7	0.28
Gang–Karr	1.01	±0.35	1.2	3.1	1.6	±0.90	1.2	1.7
Gang–Kidr	–0.75	±0.38	5.7	1.97	–0.28	±0.71	5.7	0.39
Gang–Stor	0.55	±0.36	5.4	1.52	0.80	±0.53	5.4	1.50
Gran–Karr	–0.99	±0.38	0.6	2.60	–1.10	±0.90	0.6	1.22
Gran–Kidr	–0.39	±0.23	4.5	1.69	–0.33	±0.60	4.5	0.55
Gran–Stor	0.68	±0.46	5.0	1.47	0.46	±0.80	5.0	0.57
Karr–Kidr	–1.04	±0.29	5.1	3.58	–1.40	±1.01	5.1	1.38
Kidr–Stor	–0.53	±0.28	2.3	1.89	–1.21	±0.45	2.3	2.68
Knip–Oskarshamn					1.52	±0.50	54.5	3.04

Table 8-3. Change rates of 21 dependent baseline lengths for the Äspö network. The estimated rates and their precisions are obtained from the Bernese software with the accuracies rescaled by a factor 10.

Baseline	Rate (mm/yr)	Accuracy (mm/yr)	Length (km)	$\lvert t \rvert = \frac{\hat{b}}{\hat{\sigma}_b}$
Knip–Djup	0.2	±0.6	3.5	0.3
Knip–Kidr	–0.9	±0.2	4.7	4.5
Knip–Gran	–0.2	±0.7	2.2	0.2
Knip–Karr	0.8	±0.5	2.1	1.6
Knip–Gang	0.0	±0.6	1.5	0.0
Knip–Stor	0.5	±0.7	4.1	0.7
Djup–Gang	0.0	±0.7	4.4	0.0
Djup–Gran	–0.1	±0.7	3.2	0.1
Djup–Karr	–0.7	±0.7	3.8	1.0
Djup–Kidr	–0.5	±0.7	1.3	0.7
Djup–Stor	1.5	±1.0	2.4	1.5
Gang–Granr	–0.2	±0.7	1.7	0.3
Gang–Karr	1.2	±0.6	1.2	2.0
Gang–Kidr	–0.7	±0.4	5.7	1.7
Gang–Stor	0.7	±0.8	5.4	0.8
Gran–Karr	–1.1	±0.2	0.6	5.5
Gran–Kidr	–0.3	±0.6	4.5	0.5
Gran–Stor	0.8	±0.6	5.0	1.3
Karr–Kidr	–1.0	±0.3	5.1	3.3
Kidr–Stor	–0.4	±0.7	2.3	0.6
Knip–Oskarshamn	1.8	±0.3	54.5	6.0

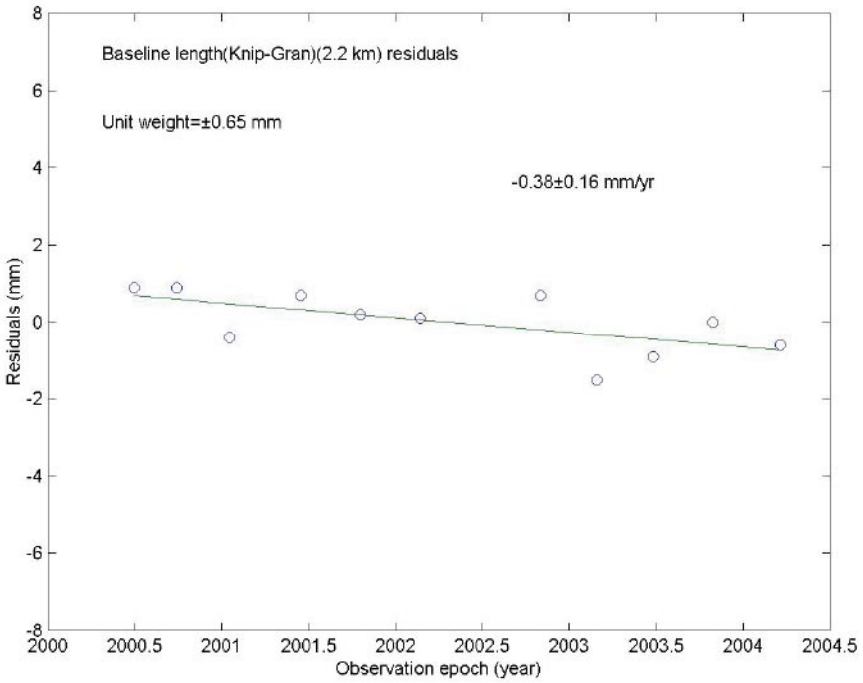

Figure 8-1. *The residuals of the baseline length Knip–Gran and the fitted line of temporal change using observable L1. Unit weight is standard error of unit weight,* σ_0.

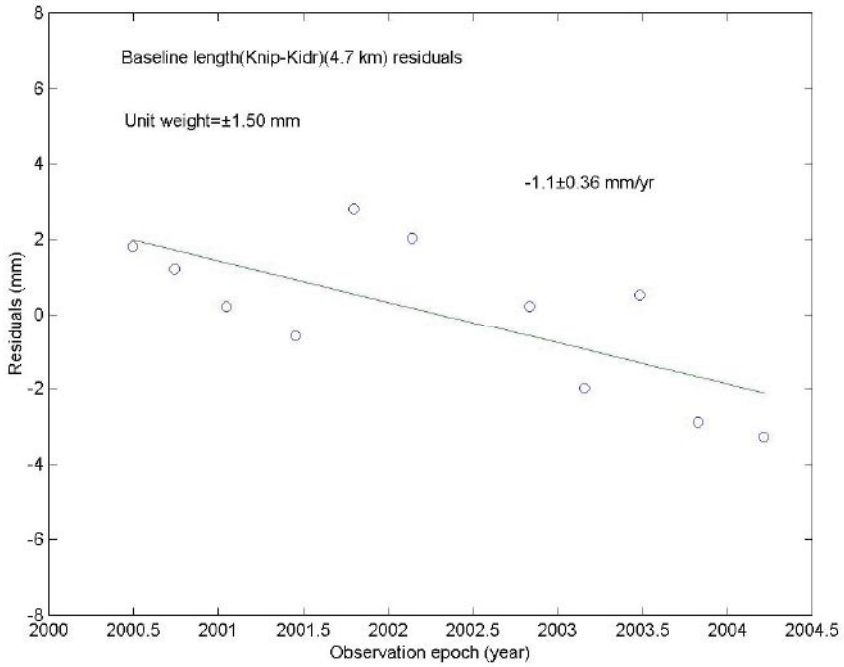

Figure 8-2. *The residuals of the baseline length Knip–Kidr and the fitted line of temporal change using observable L1. Unit weight is standard error of unit weight,* σ_0.

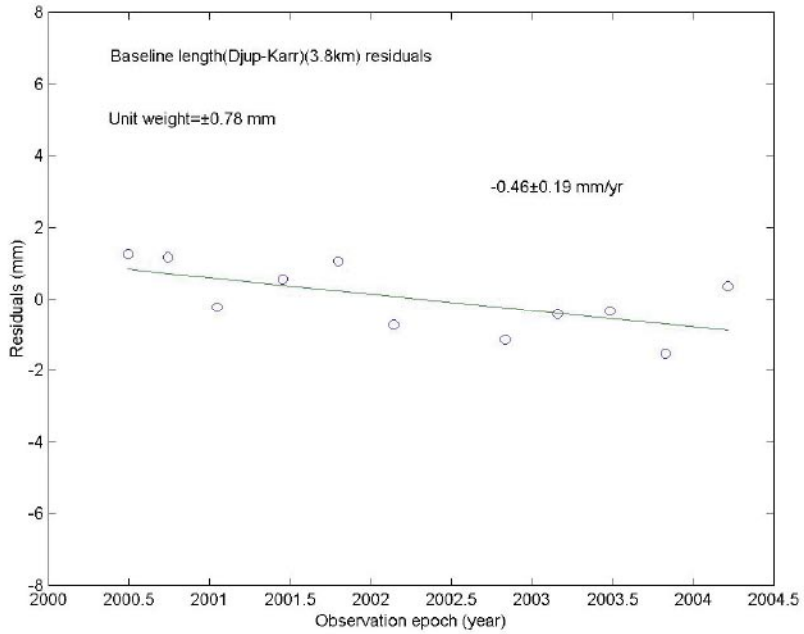

Figure 8-3. *The residuals of the baseline length Djup–Karr and the fitted line of temporal change using L1 data. Unit weight is standard error of unit weight,* σ_0.

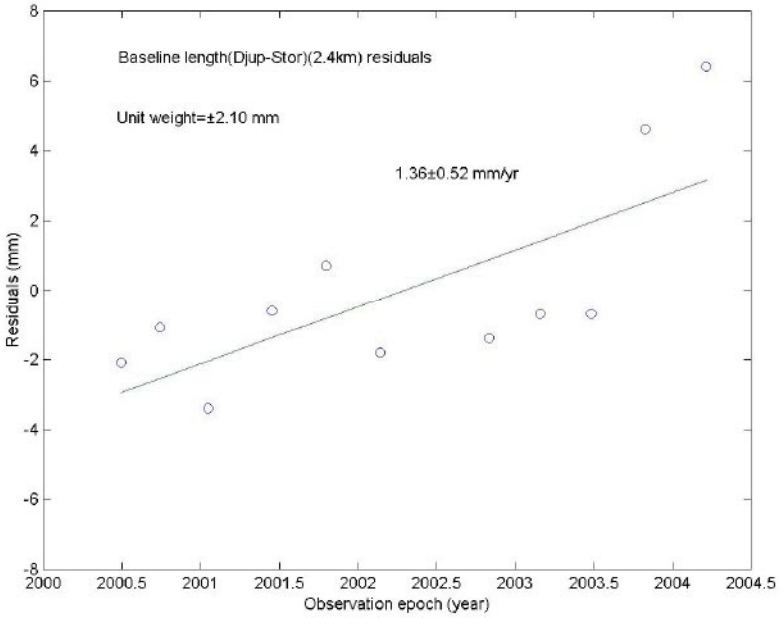

Figure 8-4. *The residuals of the baseline length Djup–Stor and the fitted line of temporal change using L1 data. Unit weight is standard error of unit weight, σ_0.*

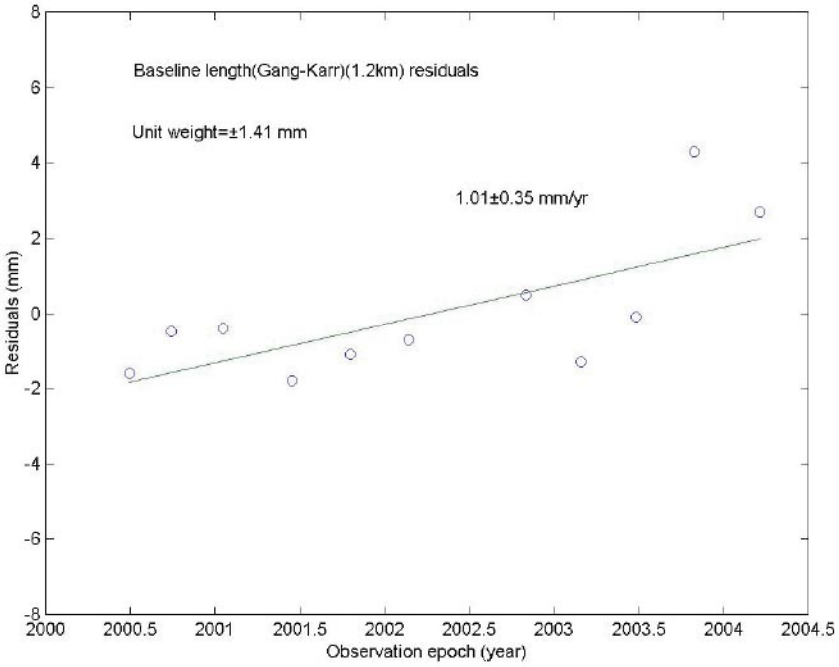

Figure 8-5. *The residuals of the baseline length Gang–Karr and the fitted line of temporal change using observable L1. Unit weight is standard error of unit weight, σ_0.*

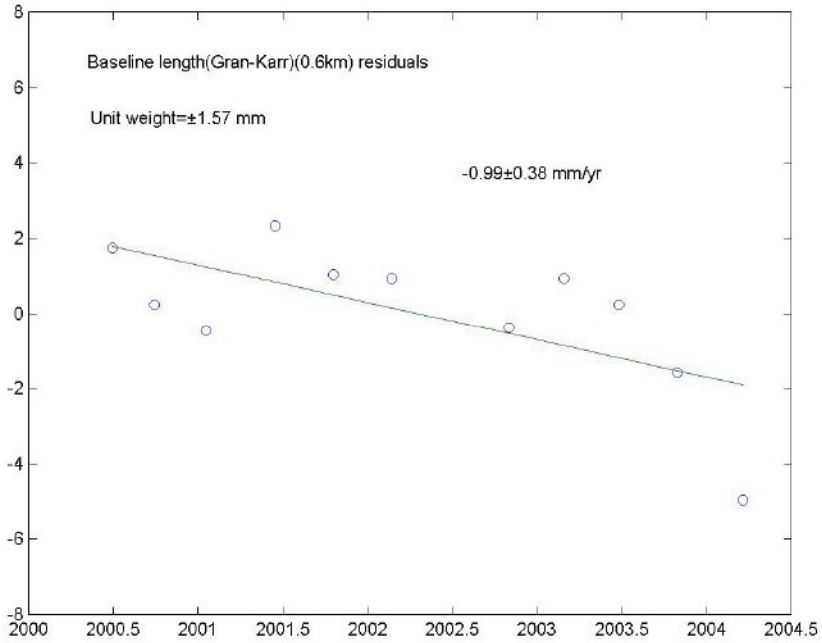

Figure 8-6. *The residuals of the baseline length Gran–Karr and the fitted line of temporal change using L1 data. Unit weight is standard error of unit weight, σ_0.*

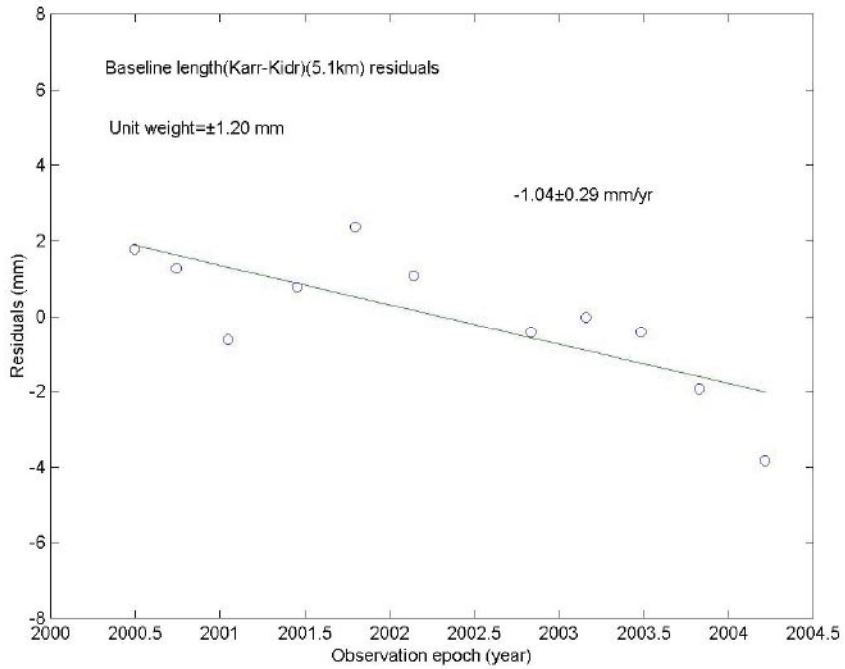

Figure 8-7. *The residuals of the baseline length Karr–Kidr and its fitted line of temporal change using observable L1. Unit weight is standard error of unit weight, σ_0.*

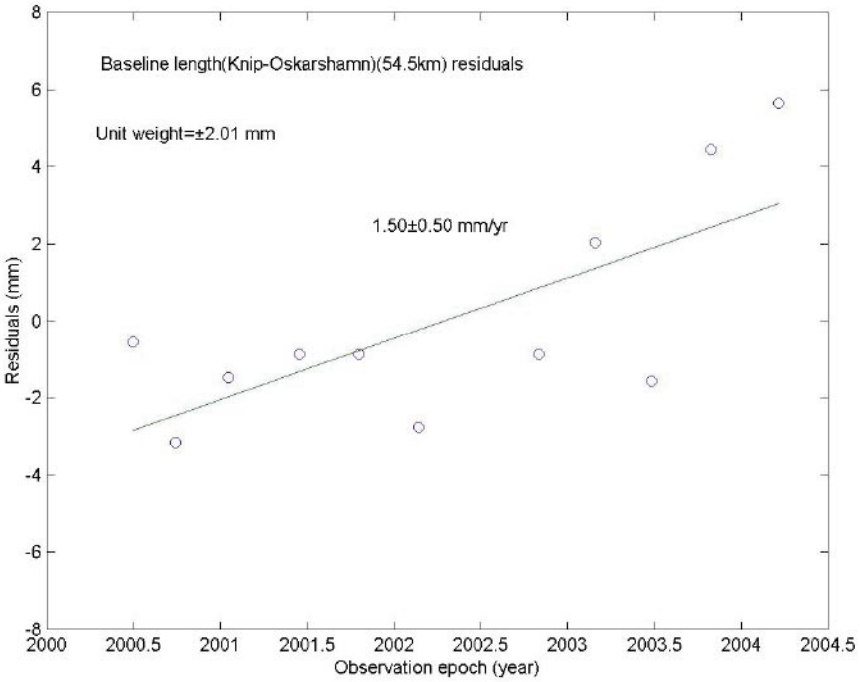

Figure 8-8. *The residuals of the baseline length Knip–Oskarshamn and the fitted line of its temporal change using observable L3. Unit weight is standard error of unit weight, σ_0.*

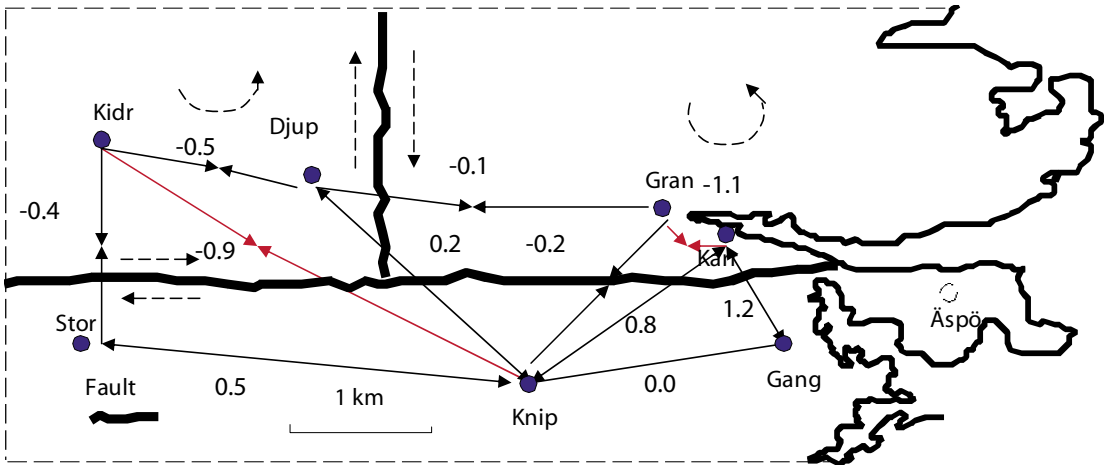

Figure 8-9. *Possible slips in mm/yr along the three blocks and rotation of two blocks estimated by the Bernese software. The red lines mean that baselines have changed significantly.*

9 Estimation of site velocities

The baseline length evolutions can only give rough information of the deformations in the network. In order to get a better overview of possible motions, the velocities of the network sites should be estimated. Therefore the site velocities were processed in a local topocentric coordinate system with respect to site Knip after the following rotations of the geocentric coordinate system:

$$\mathbf{X_{top}}=R_1(90^o-\varphi)R_3(90^o+\lambda)\mathbf{X}=\begin{pmatrix} -\sin\lambda & \cos\lambda & 0 \\ -\sin\varphi\cos\lambda & -\sin\varphi\cos\lambda & \cos\varphi \\ \cos\varphi\cos\lambda & \cos\varphi\sin\lambda & \sin\varphi \end{pmatrix}\mathbf{X}, \qquad (13a)$$

where φ and λ are the latitude and longitude of site Knip, the baseline vector $\mathbf{X=X}_{\mathbf{2}}\mathbf{-X_{knip}}$; $\mathbf{X_2}$ and $\mathbf{X_{knip}}$ are the coordinates of sites 2 and Knip in the ITRF system,

$$R_1(\varphi)=\begin{pmatrix} 1 & 0 & 0 \\ 0 & \text{con}\varphi & \sin\varphi \\ 0 & -\sin\varphi & \text{con}\varphi \end{pmatrix} \text{ and } R_3(\lambda)=\begin{pmatrix} \text{con}\lambda & \sin\lambda & 0 \\ -\sin\lambda & \cos\lambda & 0 \\ 0 & 0 & 1 \end{pmatrix} \qquad (13b)$$

The coordinates of all GPS campaigns were estimated only by phase observable L1, and the coordinates can be treated to have the same standard error (and weight) and they can be regarded as uncorrelated between epoch campaigns. Then the site velocities were estimated in two ways. In Method 1 linear regression analysis was used to estimate the coordinate rates for each coordinate and site. In Method 2 all the epoch-wise site coordinates were merged in the module ADDNEQ of the Bernese software to estimate final site coordinates and their rates. The scale factor 10, fairly in agreement with the regression analysis, was used to scale the variance factors /cf Sjöberg et al, 2002/. (The three new stations (Bast, OKG and Äspö) were not included in these analyses, as there are only one-year span of data in the three sites.)

The final 11-campaign solutions, containing the horizontal velocities and their precisions in the ITRF97, are shown in Table 9-1 (Methods 1 and 2) and Figure 9-1 (Method 2). Table 9-1 shows that only the rate of site Kidr is significant at the 95% confidence level for Method 1, while Method 2 yields 3 significant site rates of the local network (Kidr, Karr and Stor). (In addition the rate of the SWEPOS site Oskarshamn vs Knip is significant.) Figure 9-1 gives a general picture of the deformations. From these one may speculate that there are some minor translations across the faults as well as possible rotations of blocks.

The network was also tested for possible vertical crustal motions, despite of the experience that the vertical site component is 2–3 times more difficult to estimate by GPS than the horizontal ones. The estimated vertical components of the site velocities are presented in Table 9-2 and in Figures 9-2 to 9-9. From the table and the figures only one vertical site motion, 8 ± 0.6 mm/yr for site Djup, seems significant at the risk level of 5%. However, a closer look at the epoch-wise vertical component estimates (Figure 9-2) reveals that this deformation rate is not reasonable. The figure shows that, in general, the vertical component does not change significantly with time, except for a sudden jump of ca 3 cm after the third epoch campaign. The origin of this discrepancy is not known. Further data is needed to reveal whether sites Gran and Karr actually move vertically.

Decreasing the risk level to 1% only the horizontal coordinate rate of change at site Kidr is significant in the local network (both in regression analysis and Bernese adjustments). In the vertical component, site Djup is still an outlier, not satisfying the hypothesis H0.

Table 9-1. Horizontal site displacement rates of the Äspö network relative to the fixed site Knip, estimated by linear regression and by the Bernese software with precisions rescaled by a factor 10 using observable L1 (regression analysis/Bernese adjustments).

Site	Rate (mm/yr)	Precision (mm)	Azimuth	t=Rate/precision	H_0 accepted
Djup	0.51/0.37	±0.47/0.40	2°/16°	1.08/0.93	Yes
Kidr	**1.33/1.45**	**±0.41/0.40**	**173°/176°**	**3.90/3.60**	**No**
Gran	0.39/0.20	±0.25/0.40	190°/191°	1.56/0.50	Yes
Karr	0.91/1.27	±0.43/**0.40**	332°/**340°**	2.11/**3.17**	Yes/**No**
Gang	0.21/0.22	±0.20/0.40	239°/281°	1.05/0.55	Yes
Stor	1.10/1.17	±0.50/**0.40**	207°/**213°**	2.20/**2.90**	Yes/**No**
Oskarshamn	**1.60/1.89**	**±0.54//0.28**	**208°/209°**	**2.96/6.75**	**No**
t distribution (5%):2.26					

Table 9-2. Site uplift rates of the Äspö network relative to the fixed site Knip, estimated by linear regression analysis and by the Bernese software with precisions rescaled by a factor 10 (i.e. regression analysis/Bernese adjustments).

Site	Rate (mm/yr)	Precision (mm)	t=Rate/precision	H_0 accepted
Djup	8.4/7.7	±2.1/±0.6	4.0/12.8	No
Kidr	0.1/–0.35	±0.5/0.7	0.14/0.5	Yes
Gran	–1.3/**–1.8**	±0.6/**0.7**	2.16/**2.5**	Yes/**No**
Karr	–1.2/–1.6	±0.8/0.7	1.41/**2.28**	Yes/**No**
Gang	0.8/0.5	±0.5/0.7	1.70/0.7	Yes
Stor	–1.8/–1.2	±0.8/0.7	2.25/1.7	Yes
Oskarshamn	0.6/0.6	±0.6/0.8	1.00/0.7	Yes
t distribution (5%):2.26				

In Section 7.2 we adjusted the Äspö network under the assumption of no internal motions, and we compared the coordinates of these individual epoch solutions with the mean values of the coordinates in the common epoch (2002.0). The site coordinate residuals per epoch from the mean values of the eleven campaigns were listed in Tables 7-13 and 7-14. For comparison we now estimate the site component residuals and their RMS by modelling also for site motions. The results are listed in Table 9-3. Comparing with Table 7-13, it is very obvious that the residuals and their RMS values of both horizontal and vertical components have decreased after considering the site motions. This result may be another indication of possible site motions within the network.

Table 9-3. Epoch-wise coordinate residuals and their RMS values after deducting the estimated horizontal velocities of sites using L1 observable. Unit is mm.

Site	Epoch	1	2	3	4	5	6	7	8	9	10	11	RMS
Djup	North	0.6	0.5	–0.4	–1.5	1.1	1.5	–0.8	–1.9	–1.1	–1.0	3.1	1.5
	East	0.0	–0.7	–0.1	0.1	–0.8	0.7	08	1.6	–0.6	0.9	–2.0	1.0
	Up	–7.1	–7.9	–9.6	14.5	8.9	8.2	5.1	3.1	–2.2	–7.5	–5.4	8.3
Gang	North	0.7	0.3	–0.6	0.1	–0.6	0.4	–0.2	–0.8	–0.1	0.1	0.8	0.5
	East	0.2	0.2	–0.8	0.0	0.3	0.2	0.1	–0.9	0.0	0.9	–0.5	0.5
	Up	2.5	–4.3	0.8	–0.1	0.4	0.3	1.2	2.6	–2.5	–1.8	0.9	2.1
Karr	North	0.9	1.3	0.2	–0.7	–0.9	–0.6	–0.2	–2.5	–1.6	2.7	1.5	1.5
	East	0.6	–0.2	–0.7	0.3	–0.2	–0.5	0.1	1.5	–0.5	0.7	–0.9	0.7
	Up	–1.6	–2.5	–1.7	3.6	–0.4	0.5	5.2	4.9	–0.5	–4.7	–2.7	3.3
Kidr	North	0.6	–1.2	–0.5	–2.2	1.3	1.8	1.9	–0.4	2.1	–1.8	–1.5	1.6
	East	0.6	–0.3	1.0	0.2	–1.7	–1.0	0.3	1.0	–0.7	0.2	0.3	0.8
	Up	–2.8	0.8	–1.5	2.0	–1.4	3.7	1.4	0.4	1.7	–2.6	–1.7	2.1
Gran	North	0.1	0.1	–1.0	0.5	0.1	0.2	0.7	–1.2	–0.1	0.7	–0.3	0.6
	East	0.1	0.5	0.5	–0.5	–0.2	–0.8	0.6	0.2	–1.1	–0.7	1.4	0.7
	Up	–1.6	–0.3	0.1	3.3	–1.2	–2.8	2.0	4.0	0.8	–2.9	–1.3	2.3
Stor	North	–0.3	–1.0	0.5	–1.3	–0.8	2.8	0.9	1.2	1.8	–2.5	–1.3	1.6
	East	–0.1	–1.0	0.7	–1.2	–0.7	1.5	2.2	0.8	–0.2	–0.5	–1.5	1.1
	Up	–3.3	1.3	6.0	1.8	–1.1	–2.7	–1.4	–0.3	5.5	0.7	–2.8	3.2

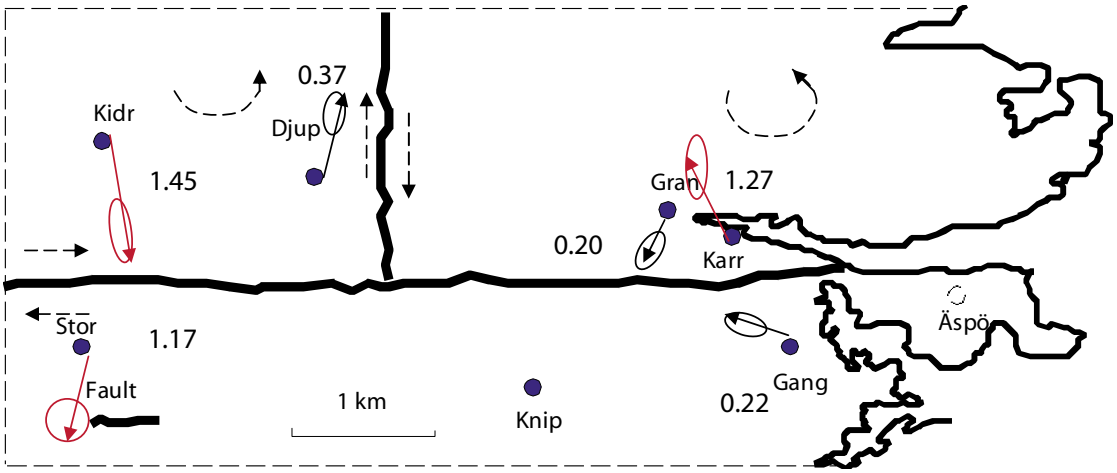

Figure 9-1. *The site motion rates in mm/yr of the Äspö network derived by the Bernese software using all the data from June 2000 to March 2004, related to the fixed site Knip. The formal error ellipses were rescaled by a factor 10 and red lines show that the site movements are significant at 95% level.*

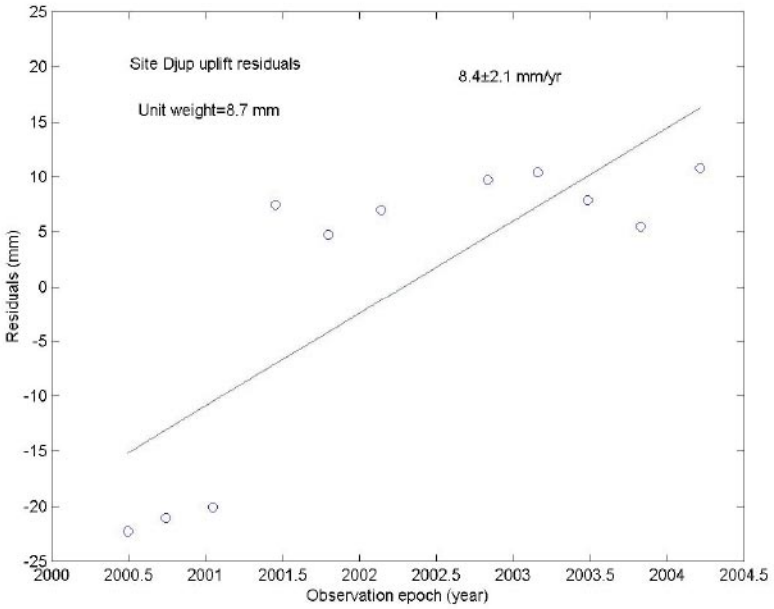

Figure 9-2. *Residuals of the vertical component at site Djup and the fitted line. Unit weight is standard error of unit weight, σ_0.*

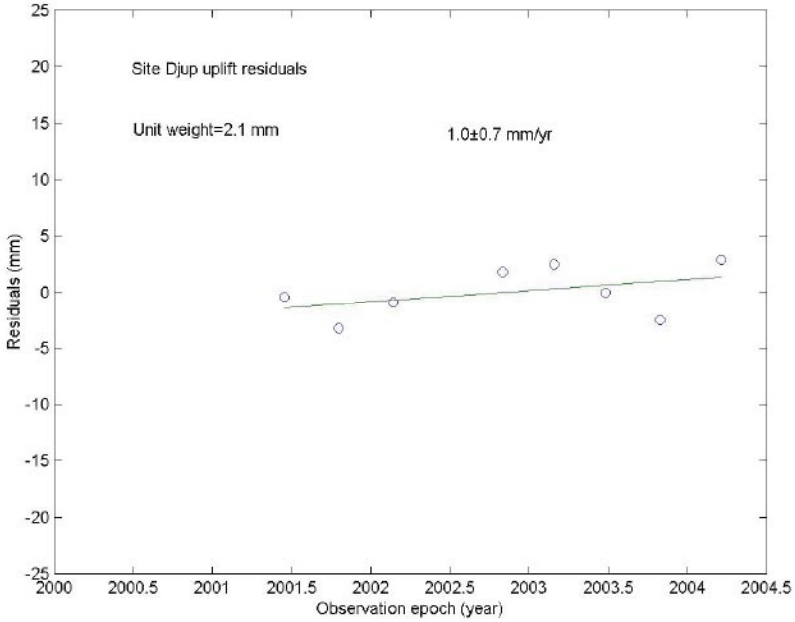

Figure 9-3. *As Figure 9-2 but without the data from the first three epochs. Unit weight is standard error of unit weight, σ_0.*

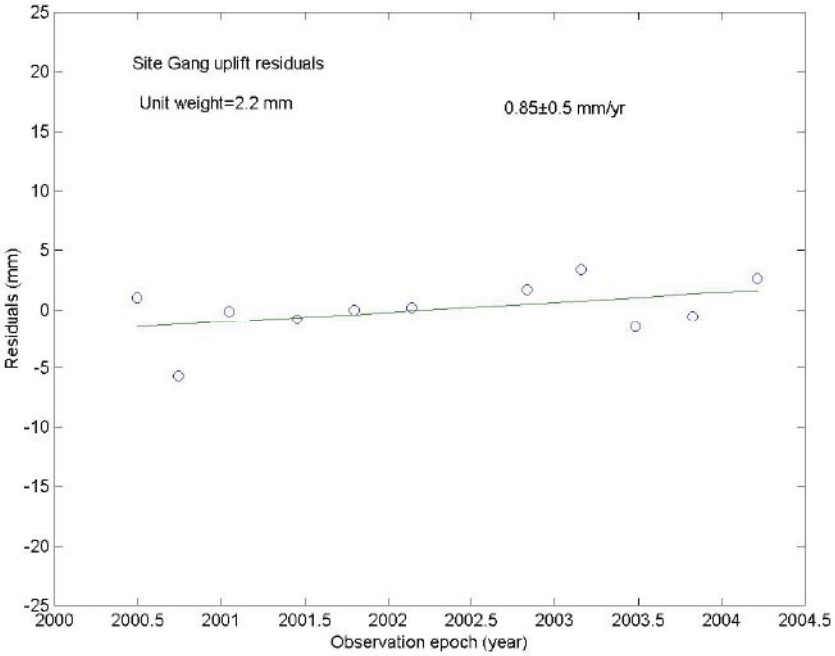

Figure 9-4. *Residuals of the vertical component at site Gang and the fitted line. Unit weight is standard error of unit weight, σ_0.*

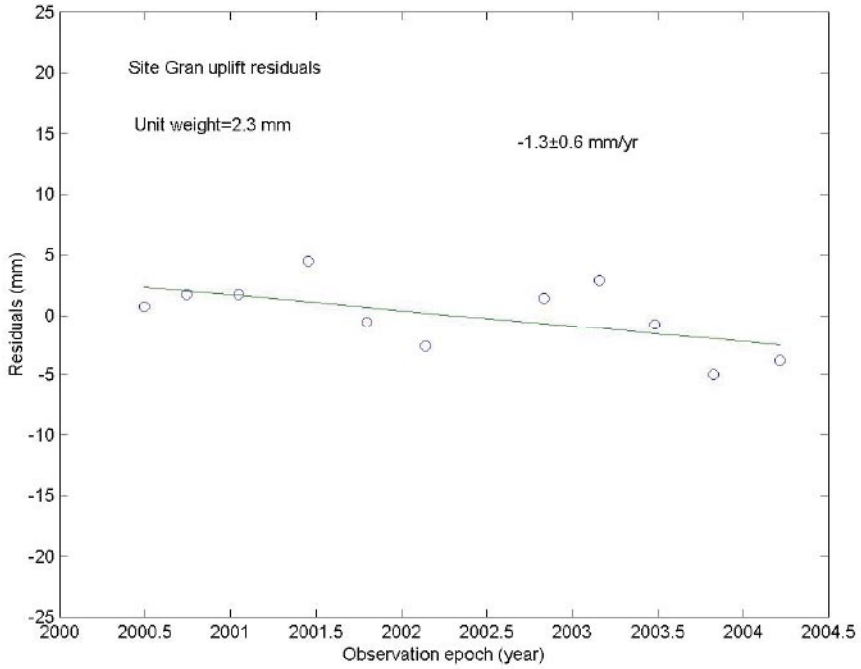

Figure 9-5. *Residuals of the vertical component at site Gran and the fitted line. Unit weight is standard error of unit weight, σ_0.*

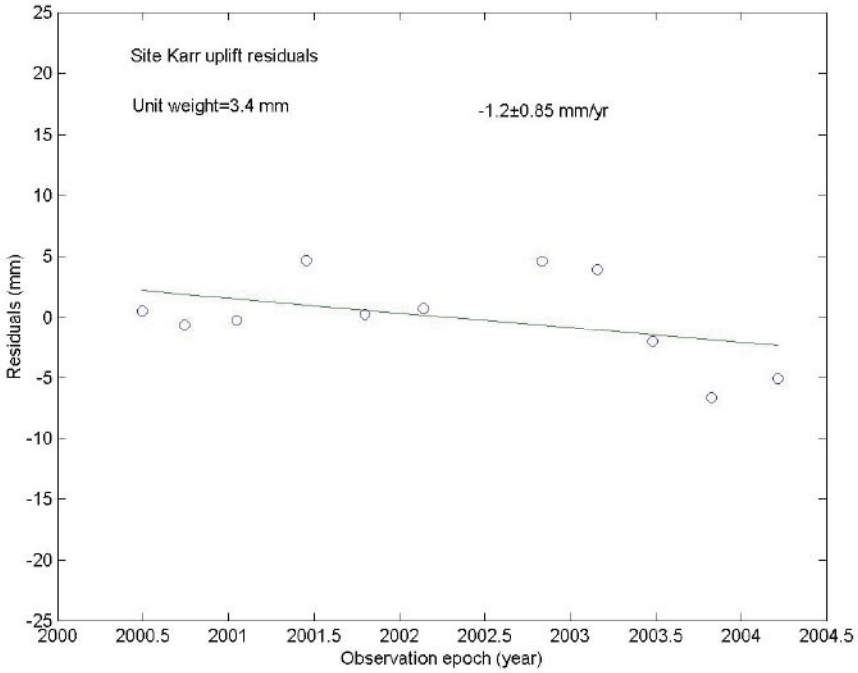

Figure 9-6. *Residuals of the vertical component at site Karr and the fitted line. Unit weight is standard error of unit weight, σ_0.*

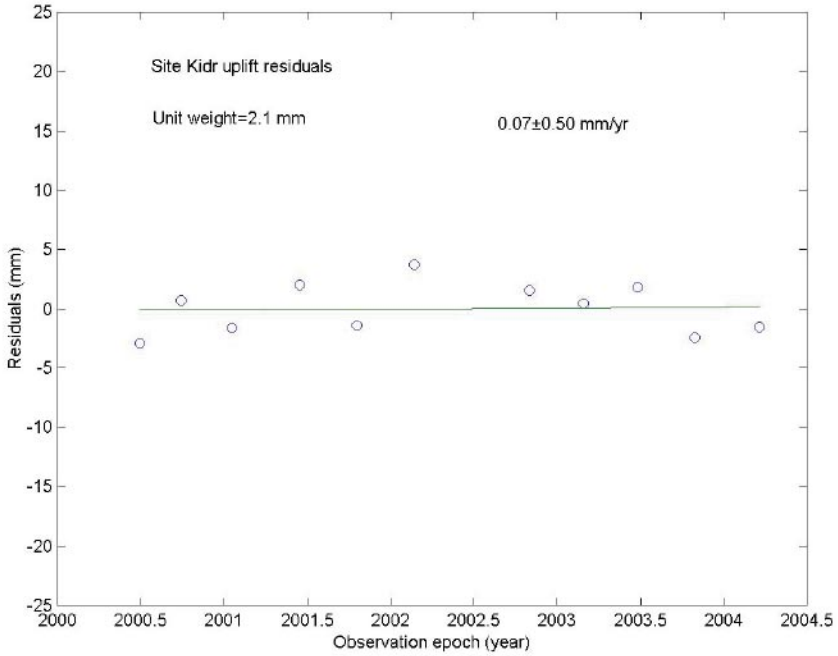

Figure 9-7. *Residuals of the vertical component at site Kidr and the fitted line. Unit weight is standard error of unit weight, σ_0.*

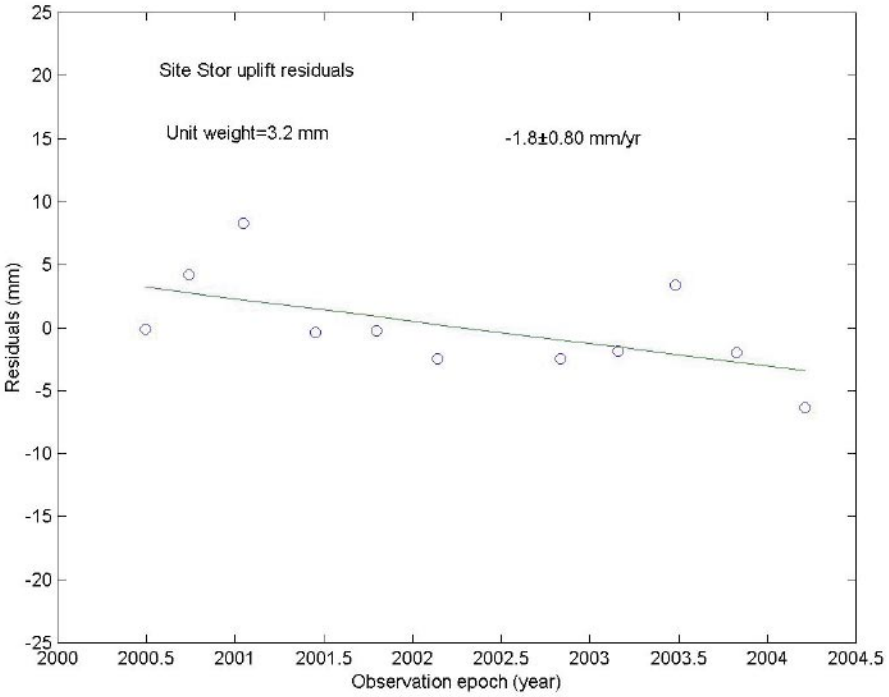

Figure 9-8. *Residuals of the vertical component at site Stor and the fitted line. Unit weight is standard error of unit weight, σ_0.*

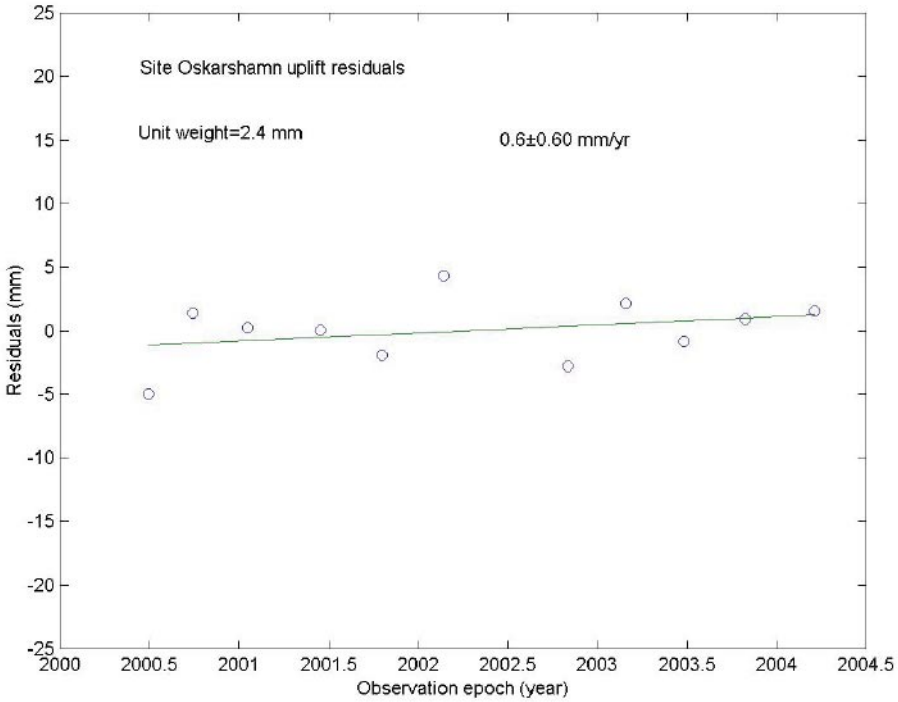

Figure 9-9. *Residuals of the vertical component at site Oskarshamn and the fitted line. Unit weight is standard error of unit weight, σ_0.*

10 Discussion and final conclusions

Since its establishment in the year of 2000 the Äspö GPS monitoring network has been repeatedly observed during eleven epoch GPS campaigns. Unfortunately, during this time interval the 11-year cycle of the solar activity, causing well-known ionospheric signal disturbances, reached its maximum. The ionosphere activity was rather strong during all observation campaigns, reaching a maximum at the end of 2002. Also, in October 30, 2003, during the tenth GPS campaign, the sunspot activity was severe and it strongly deteriorated some of the observation data. Under normal circumstances the ionosphere bias is not a problem to small network adjustments, as it is efficiently reduced by differencing and modelling of the L1 and L2 observables, and only L1 is used as the direct observable together with the ionosphere model in the network adjustment. Due to the strong ionosphere activity we now decided to test both the L1 and L3 (the ionosphere-free linear combination) GPS observables for the network adjustment. Normally the result of L3 is noisier (i.e. it has larger standard errors), and its reduction of possible ionosphere bias is not an advantage for a small-scale network. Surprisingly, the preliminary, static adjustment showed worse daily repeatability of horizontal components estimated by the L1 data compared to those estimated by L3 data (cf Tables 7-2 to 7-11). However, in contrast, the linear regression of the baseline lengths showed worse results for L3 vs L1 (see Table 8-2). This somewhat controversial result can be explained as follows. The first test concerned the repeatability of the GPS results from session to session during each campaign. It usually implies that the GPS antenna is not moved between sessions. The second test concerned the fitting of the baseline results from all epoch campaigns. It is obvious that in the second test more error sources, not significant when comparing sessions within a campaign, are relevant. For example, the exchange of antennas from one campaign to another will lead to different antenna calibration errors, not present in the first test. (The L3 observable is more prone to this type of error than L1.) This comparison convinced us to use the L1 data with a global ionosphere model determined from L1 and L2 data for the final analysis of the deformation network. (Actually, the result of an analysis based on L3 agrees rather well with that on L1 despite of being noisier.)

The standard errors of baseline and coordinate velocities based on real data are usually somewhat bigger than their theoretical estimates (cf Tables 8-1, 8-2 and 9-1). First of all, the theoretical estimates assume no systematic errors in the data. The actual outcome may indicate the presence of some systematic error sources such as ionosphere residual bias and antenna calibration errors, but also other local systematic error sources might prevail. Long observation periods are needed to control such systematic error resources. The antenna calibration error can be controlled by strictly using the same antenna at each site and campaign.

Nevertheless, the analysis of all the GPS data shows that there is some information of possible deformations in the local network. At the risk level of 5% (1%) the regression analysis of baseline lengths reveals that 7 (1) out of 20 dependent baselines have significant change rates. As an alternative, the Bernese software adjustment (using a standard error scaling factor of 10) yields 3 significant baseline rates at both risk levels. They are Knip–Kidr (–0.9 ±0.2 mm/yr), Gran–Karr (–1.1 ± 0.2 mm/yr) and Karr–Kidr (–1.0 ± 0.3 mm/yr). These numbers are outstanding among the baseline rate estimates not only for relatively large change rates but also for their small standard errors.

At the risk level of 5% the estimation of the horizontal site motions vs the fixed station Knip, using a joint deformation analysis from all the data by the Bernese program, yields that three sites have moved: site Kidr moves to the SSE at the rate of 1.5 mm/yr, site Stor moves to the SSV at 1.2 mm/yr and site Karr moves to the NV at 1.3 mm/yr. The standard error is 0.4 mm/yr for all these estimates. The remaining three sites are stable (with respect to Knip). These results might be interpreted as counter-clockwise rotations of the two blocks, but this result is not confirmed by the present data.

For the risk level of 1% only site Kidr shows a motion. A special study of the vertical site motions show small changes. However, the epoch-wise vertical components for site Djup show an abnormal jump of ca 30 mm between two epoch campaigns. We have no explanation to this sudden discrepancy.

As the possible deformations in the Äspö area are small, one can only get some rough information about these phenomena in four years time. Unfortunately, the GPS data was collected close to the time of solar maximum, which inevitably, despite of modelling, must have corrupted the data by some ionosphere bias. The remaining bias may also have influenced the estimated time evolution of the network baselines and coordinates. Fortunately, the ionosphere activity will calm down after 2004, which certainly will improve data quality of possible near future GPS campaigns. To fully explore the possible influence of the ionosphere bias, the observation period should be extended, possibly to cover a full period of the solar cycle. As the total observation period (T) is more important for the estimation of temporal variations of parameters than the number of observation campaigns each year (n), it should be advantageous to extend T and, possibly, reduce n to two instead of three as has been the case up to now. (In any possible future GPS campaigns it will be possible to eliminate the antenna calibration error, as KTH has now achieved a sufficient number of choke ring antennas by a generous donation from Knut and Alice Wallenberg’s Foundation.)

References

Becker M, Reinhart E, Nordin S B, Angemann D, Michel C, Reigber C, 2000. Improving the velocity field in South and south-east Asia: The third round of GEODYSSEA. Earth Planets Space, 52, pp 721–726.

Boucher C, Altamimi Z, Sillard P, 1999. The 1997 International Terrestrial Reference Technical note No 27, Observatories de Paris.

Bjerhammar A, 1973. Theory of errors and generalized matrix inverses. Elsevier Scientific Publishing Co., Amsterdam, London, New York.

Brekke P, 2003. SOHO's Role as a Space Weather Watchdog, Nordic Space Activities, Vol. 11, pp 6–8.

Fridez P, 2002. Private communication, Astronomical Institute, University of Berne.

Hedling G, Jonsson B, 1995. SWEPOS-A Swedish Network of Reference Stations for GPS. LMV-rapport 1995:15, Gävle, Sweden.

Hugentobler U, Schaer S, Fridez P (Ed.), 2001. Bernese GPS Software, Version 4.2, Astronomical Institute University of Berne, February 2001.

Koch K R, 1999. Parameter Estimation and Hypothesis Testing in Linear Models, Second updated and enlarged Edition. Springer-Verlag, Berlin, Heidelberg.

Rothacher M, Mervart L, Beutler G, Brockhamn E, Fankhauser S, Gurtner W, Johnsson J, Schaer S, Springer T, Weber R, 1996. Manual for Bernesr GPS Software Version 4.0. Astronomical Institute University of Berne.

Schaer S, 1998. Code's Global Ionosphere Maps (GIMs), http://www.aiub.unibe.ch/ionosphere, html, automatically updated web site.

Sillard P, Boucher P, 2001. A review of algebraic constrints in terrestrial refernce frame datum definition. J. Geod., 75, 63–73.

Sjöberg L E, 1982. Singular versus regular adjustment of gravity networks for various observation strategies. The Department of Geodesy Report No 15, University of Uppsala.

Sjöberg L E, 1984. General matrix calculus, adjustment and variance-covariance component estimation. In B. Harsson (Ed.): Optimization of Geodetic operations, Lecture Notes, Nordiska Forskarkurser 12/1984, Norges Geografiske Oppmåling Publ. No 3/1984, pp 7–69.

Sjöberg L E, Pan M, Asenjo E, 2002. An analysis of the Äspö crustal motion-monitoring network observed by GPS in 2000, 2001, and 2002, R-02-33, Svensk Kärnbränslehantering AB.

SKB, 2000. Förstudie Oskarshamn, slutrapport.

SKB, 2001a. Platsundersökningar. Undersökningsmetoder och generellt genomförandeprogram. SKB R-01-10, Svensk Kärnbränslehantering AB.

SKB, 2001b. Geovetenskapligt program för platsundersökning vid Simpevarp. SKB R-01-44, Svensk Kärnbränslehantering AB.

Spilker J, 1978. GPS Signal Structure and Performance Characteristics, Navigation, The Journal of the Institute of Navigation, Washington, Vol. 25, No 2 pp121–146.